Controls on spatial and temporal variability of streamflow and hydrochemistry in a glacierized catchment

Running title: Controls on streamflow and hydrochemistry in a glacierized catchment

Michael Engel[1], Daniele Penna[2], Giacomo Bertoldi[3], Gianluca Vignoli[4], Werner Tirler[5,] and Francesco Comiti[1]

[1]Faculty of Science and Technology, Free University of Bozen-Bolzano, Piazza Università 5, 39100 Bozen-Bolzano, Italy

[2] Department of Agriculture, Food, Environment and Forestry (DAGRI)

University of Florence, Via S. Bonaventura, 13, University of Florence, 50145 Florence, Italy

[3]Institute for Alpine Environment, Eurac Research, Viale Druso 1, 39100 Bozen-Bolzano, Italy

[4]CISMA S.r.l., Via Volta 13/A, 39100 Bozen-Bolzano, Italy

[5]Eco-Research S.r.l., Via Negrelli 13, 39100 Bozen-Bolzano, Italy

Correspondence to: Michael Engel (Michael.Engel@unibz.it)

Abstract

Understanding the hydrological and hydrochemical functioning of glacierized catchments requires the knowledge of the different controlling factors and their mutual interplay. For this purpose, the present study was carried out in two sub-catchments of the glacierized Sulden River catchment (130 km², Eastern Italian Alps) in 2014 and 2015, characterized by similar size but contrasting geological setting. Samples were taken at different space and time scales for analysis of stable isotopes in water, electrical conductivity, major, minor and trace elements.

At the monthly sampling scale, complex spatial and temporal dynamics for different spatial scales (0.05 – 130 km²) were found, such as contrasting electrical conductivity gradients in both sub-catchments. At the daily scale, for the entire Sulden catchment the relationship between discharge and electrical conductivity showed a monthly hysteretic pattern. Hydrometric and geochemical dynamics were controlled by an interplay of meteorological conditions, topography and geological heterogeneity. A principal component analysis

revealed that the largest variance (36.3 %) was explained by heavy metal concentrations (such as Al, V, Cr, Ni, Zn, Cd, Pb) during the melting period while the remaining variance (16.3 %) resulted from the bedrock type in the upper Sulden sub-catchment (inferred from electrical conductivity, Ca, K, As and Sr concentrations). Thus, high concentrations of As and Sr in rock glacier outflow may more likely result from bedrock weathering. Furthermore, nivo-meteorological indicators such as daily maximum air temperature and daily maximum global solar radiation represented important meteorological controls, with significant snowmelt contribution when exceeding 5 °C or 1000 W m^{-2}, respectively. These insights may help to better understand and predict hydrochemical catchment responses linked to meteorological and geological controls and to guide future classifications of glacierized catchments according to their hydrochemical characteristics.

1 Introduction

Runoff from glacierized catchments is an important fresh water resource to downstream areas (Kaser et al., 2010; Viviroli et al., 2011). High-elevation environments face rapid and extensive changes through retreating glaciers, reduced snow cover, and permafrost thawing (Harris et al., 2001; Dye, 2002; Beniston, 2003; Galos et al., 2015). This will have impacts on runoff seasonality, water quantity and water quality (Beniston 2006; Ragettli et al., 2016; Gruber et al., 2017; Kumar et al., 2018). Therefore better understanding the behaviour of high-elevation catchments and their hydrological and hydrochemical responses at different spatial and temporal scales is of uttermost importance in view of water management, water quality, hydropower, and ecosystem services under the current phase of climate change (Beniston, 2003; Viviroli et al., 2011; Beniston and Stoffel, 2014).

In general, the hydrological response of catchments (i.e., runoff dynamics) is controlled by heterogeneous catchment properties (Kirchner, 2009), which become more diverse in catchments with large complexity of various landscape features, as it is the case of mountainous, high-elevation glacierized catchments (Cook and Swift, 2012). In fact, those catchments are deemed as highly dynamic geomorphological, hydrological and biogeochemical environments (Rutter et al., 2011). The advances on tracer and isotope hydrology made during the last decades can substantially contribute to gain more insights into the variability of different runoff components of high-elevation catchments (Vaughn and

Fountain, 2005; Maurya et al., 2011; Xing et al., 2015; Penna et al., 2017b), catchment conceptualization (Baraer et al., 2015; Penna et al., 2017a), and sensitivity to climate change (Kong and Pang, 2012).

The main controls on hydrological and hydrochemical catchment responses are represented by climate, bedrock geology, surficial geology, soil, vegetation, topography, drainage network (Devito et al., 2005; Williams et al 2015) and catchment shape (Sivapalan 2003). These catchment properties may affect the partitioning of incoming water and energy fluxes (Carrillo et al., 2011).

First, a major role is attributed to the global and regional climate, having strong impacts on mountain glaciers and permafrost, streamflow amount and timing, water quality, water temperature, and suspended sediment yield (Milner et al., 2009; Moore et al., 2009; IPCC, 2013). The impact of climate is difficult to assess because it requires long time windows (e.g., decades), whereas meteorological drivers interact at a smaller temporal scales and thus are easier to quantify. Among different meteorological drivers, radiation fluxes at the daily time scale were identified as main energy source driving melting processes in glacierized catchments in different climates (Sicart et al., 2008). Beside radiation, air temperature variations generally correlate well with streamflow under the presence of snow cover (Swift et al., 2005) and may affect the daily streamflow range (Penna et al., 2016; Zuecco et al., 2018) and streamflow seasonality (Hock et al, 1999; Cortés et al., 2011) only after an air temperature threshold has been reached.

Geology sets the initial conditions for catchment properties (Carrillo et al., 2011). The geological setting strongly controls catchment connectivity, drainage, and groundwater discharge (Farvolden 1963), runoff response (Onda et al., 2001), residence time (Katsuyama et al., 2010), hydrochemistry during baseflow conditions (Soulsby et al., 2006a) and melting periods (Hindshaw et al., 2011), and subglacial weathering (Brown and Fuge, 1998). Also geomorphological features such as talus fields may affect streamflow and water quality, resulting from different flow sources and flow pathways (Liu et al., 2004). Catchment storage, as determined by both geology and topography, was found to impact the stream hydrochemistry as well (Rinaldo et al., 2015).

The catchment hydrological conditions, commonly referring to the antecedent soil moisture, are also a relevant driver of the hydrological response (Uhlenbrook and Hoeg, 2003; Freyberg et al., 2017). Specifically in high elevation and high latitude catchments, also permafrost

thawing affects the hydrological connectivity (Rogger et al., 2017), leading to a strong control on catchment functioning as it drives the partitioning, storage and release of water (Tetzlaff et al., 2014). In more detail, retreating permafrost may also result in distinct geochemical signatures (Clark et al., 2001; Lamhonwah et al., 2017) and the release of heavy metals being previously stored in the ice (Thies et al., 2007; Krainer et al., 2015). As those contaminants do not affect only the water quality but also the aquatic biota such as macroinvertebrate communities in high elevation and high latitude environments (Milner et al., 2009), the hydrochemical characterization of permafrost thawing (i.e., from rock glaciers as a specific form of permafrost) and its impact on stream hydrology deserves further investigation (e.g. Williams et al., 2006, Carturan et al., 2015; Nickus et al. 2015; Colombo et al. 2017).

Although the effect of catchment characteristics and environmental conditions on stream hydrochemistry at different spatial and temporal scales has been well studied in lowland and mid-land catchments (e.g., Wolock et al., 1997; McGuire et al. 2005; Tetzlaff et al., 2009), only few studies have focused on this aspect in glacierized or permafrost-dominated catchments (Wolfe and English, 1995; Hodgkins, 2001; Carey and Quinton 2005; Lewis et al., 2012; Kumar et al., 2018). In fact, investigating the geological, meteorological, and topographic controls on catchment response and stream water hydrochemistry in high-elevation catchments is essential when analyzing the origin of hydrochemical responses in larger catchments (Chiogna et al., 2016; Natali et al., 2016), calibrating hydrological models (Weiler et al., 2017) and analysing catchment storages (Staudinger et al., 2017).

In this paper, we aim to fill this knowledge gap by analysing hydrochemical data from a two-year monitoring campaign in two nearby glacierized catchments in the Eastern Italian Alps, characterized by similar size and climate but contrasting geological setting. We hypothesise that the markedly different geological properties affect the geochemistry and the hydrological response of both catchments. We test this hypothesis by sampling different water sources (precipitation, stream water, groundwater, snowmelt, and glacier melt) for the electrical conductivity (EC), turbidity, major, minor and trace elements analysis.

Within the present study, we specifically aim to answer the following research questions:

- Does the temporal pattern of the hydrochemical stream signature in the two catchments reflect the dominant rock substratum?

- Do nivo-meteorological indicators (precipitation, air temperature, solar radiation, snow depth) impact the stream hydrochemical response during the melting period?
- What is the temporal relationship of discharge and tracer characteristics in the stream?

2 Study area and instrumentation

2.1 The Sulden River catchment

The study was carried out in the Sulden/Solda River catchment, located in the upper Vinschgau/Venosta Valley (Eastern Italian Alps) (Fig. 1). The size of the study area is about 130 km² defined by the stream gauge station of the Sulden River at Stilfserbrücke/ Ponte Stelvio (1110 m a.s.l.), with a mean elevation of 2507 m a.s.l.. The highest elevation is represented by the Ortler/ Ortlers peak (3905 a.s.l.) within the Ortles-Cevedale group. A major tributary is the Trafoi River, joining the Sulden River close to the village Trafoi-Gomagoi. At this location, two sub-catchments, namely Sulden and Trafoi sub-catchment (75 and 51 km², respectively) meet.

The study area had a glacier extent of about 16.9 km² (13 % of the study area) in 2011, which is slightly higher in the Trafoi than in the Sulden sub-catchment (16.5 % and 11.1 %, respectively). Main glacier tongues in the study area are represented by the Madatsch glacier (Trafoi sub-catchment) and Sulden glacier (Sulden sub-catchment). Geologically, the study area belongs to the Ortler-Campo-Cristalin (Mair et al., 2007). While permotriassic sedimentary rocks dominate the Trafoi sub-catchment, Quarzphyllite, Orthogneis, and Amphibolit are present in the Sulden sub-catchment. However, both catchments share the presence of orthogneis, paragneis and mica schist from the lower reaches to the outlet. Permafrost is discontinuously located between 2400 and 2600 m a.s.l. and continuously above 2600 m a.s.l. (Boeckli et al., 2012). Available climatological data show a mean annual air temperature of about -1.6 °C and a mean annual precipitation of about 1008 mm (2009 - 2016) at 2825 m a.s.l. (Hydrographic Office, Autonomous Province of Bozen-Bolzano). Due to the location of the study area in the inner dry Alpine zone, these precipitation amounts are relatively low compared to the amounts at similar elevation in the Alps (Schwarb, 2000). Further climatic data regarding the sampling period of this study are shown in Table 1.The study area lies within the National Park “Stelvio / Stilfser Joch” but it also includes ski slopes and infrastructures, as well as hydropower weirs.

2.2 Meteorological, hydrometric and topographical data

Precipitation, air temperature, humidity and snow depth are measured by an ultrasonic sensor at 10 min measuring interval at the automatic weather station (AWS) Madritsch/Madriccio at 2825 m a.s.l., run by the Hydrographic Office, Autonomous Province of Bozen-Bolzano (Fig. 1). We take data from this station as representative for the glacier in the catchment at similar elevation. At the catchment outlet at Stilfserbrücke/Ponte Stelvio, water stages are continuously measured by an ultrasonic sensor (Hach Lange GmbH, Germany) at 10 min measuring interval and converted to discharge via a flow rating curve using salt dilution/photometric measurements (measurement range: 1.2 – 23.2 $m^3 s^{-1}$; n = 22). Turbidity is measured by a SC200 turbidity sensor (Hach Lange GmbH, Germany) at 5 min measuring interval, which was resampled to 10 min time steps. All data used in this study are recorded and presented in solar time.

Topographical data (such as catchment area and 50 m elevation bands) were derived from a 2.5 m digital elevation model.

2.3 Hydrochemical sampling and analysis

Stream water sampling at the outlet was performed by an automatic sampling approach using an ISCO 6712 system (Teledyne Technologies, USA). Daily water sampling took place from mid-May to mid-October 2014 and 2015 (on 331 days, mainly during melt water conditions) at 23:00 to ensure consistent water sampling close to the discharge peak. In addition, grab samples were taken from different stream locations, tributaries, and springs in the Sulden and Trafoi sub-catchments and the outlet, following the sampling scheme of Penna et al. (2014) to account for spatial variability of the hydrochemistry at the catchment scale. Sampling took place monthly from February 2014 to November 2015 (Table 2). Samples were collected approximately at the same time (within less than an hour of difference) on all occasions. In winter, however, a different sampling time had to be chosen for logistical constraints (up to four hours of difference between both sampling times). However, this did not produce a bias on the results due to the very limited variability of the hydrochemical signature of water sources (related to nearly-constant discharge) during winter baseflow conditions (Immerzeel et al., 2012). Three outflows from two active rock glaciers were selected to represent meltwater from permafrost because rock glaciers are considered as long term creeping ice-

184 rock mixtures under permafrost conditions (Humlum 2000). Located on Quarzphyllite
185 bedrock in the upper Sulden sub-catchment, three springs at the base of the steep rock glacier
186 front at about 2600 m a.s.l. were sampled monthly from July to September 2014 and July to
187 October 2015. Snowmelt water was collected as dripping water from snow patches from April
188 to September 2014 and March to October 2015 (n = 48 samples), mainly located on the west
189 to north-facing slopes of the Sulden sub-catchment and at the head of the valley in the Trafoi
190 sub-catchment. Glacier melt water was taken from rivulets only at the eastern tongue of the
191 Sulden glacier from July to October 2014 and 2015 (n = 11 samples) for its safe accessibility.
192 EC was measured in the field by a portable conductivity meter WTW 3410 (WTW GmbH,
193 Germany) with a precision of +/- 0.1 µS cm^{-1} (nonlinearly corrected by temperature
194 compensation at 25 °C).
195 All samples were stored in 50 ml PVC bottles with a double cap and no headspace. The
196 samples were kept in the dark at 4°C in the fridge before analysis. δ^2H and $\delta^{18}O$ isotopic
197 composition of all water samples (except the ISCO stream water samples at the outlet) were
198 analysed at the Laboratory of Isotope and Forest Hydrology of the University of Padova
199 (Italy), Department of Land, Environments, Agriculture and Forestry by an off-axis integrated
200 cavity output spectroscope (model DLT-100 908-0008, Los Gatos Research Inc., USA). The
201 analysis protocol and the description of reducing the carry-over effect are reported in (Penna
202 et al., 2010, 2012). The instrumental precision (as an average standard deviation of 2094
203 samples) is 0.5‰ for δ^2H and 0.08‰ for $\delta^{18}O$.
204 The $\delta^{18}O$ isotopic composition of the ISCO stream water samples was analysed by an isotopic
205 ratio mass spectrometer (GasBenchDelta V, Thermo Fisher) at the Free University of Bozen-
206 Bolzano. Following the gas equilibration method (Epstein and Mayeda, 1953), 200-µl sub-
207 samples were equilibrated with He–CO_2 gas at 23 °C for 18 h and then injected into the
208 analyser. The isotopic composition of each sample was calculated from two repetitions, and
209 the standard deviation was computed. The instrumental precision for $\delta^{18}O$ was ±0.2‰. We
210 applied a correction factor, described in Engel et al. (2016), to adjust the isotopic
211 compositions of $\delta^{18}O$ measured by the mass spectrometer to the ones measured by the laser
212 spectroscope.
213 The analysis of major, minor and trace elements (Li, B, Na, Mg, Al, K, Ca, V, Cr, Mn, Fe,
214 Co, Ni, Cu, Zn, Rb, Sr, Mo, Ba, Pb and U) was carried out by Inductively Coupled Plasma

Mass Spectroscopy (ICP-MS ICAP-Q, Thermo Fischer) at the laboratory of EcoResearch srl. (Bozen-Bolzano).

2.4 Data analysis

In order to better understand the effect of meteorological controls at different time scales, different nivo-meteorological indicators derived from precipitation, air temperature, solar radiation and snow depth data from AWS Madritsch were calculated (Table 3).

We performed a temporal sensitivity analysis to better understand at which temporal scale these nivo-meteorological indicators affect the hydrometric and hydrochemical stream response at the outlet. For that purpose, we calculated the indicators for each day of stream water sampling and included in the calculations a period of time of up to 30 days prior to the sampling day by using a one day incremental time step. As precipitation indicators, we considered the cumulated precipitation P in a period between 1 and 30 days prior to the sampling day, and the period of time D_{prec} in days starting from 1, 10 or 20 mm of cumulated precipitation occurred prior to the sampling day. We selected the daily maximum air temperature T_{max} and daily maximum global solar radiation G_{max} in a period between 1 and 30 days prior the sampling day as snow and ice melt indicators. Moreover, we calculated the difference of snow depth, ΔSD, and used it as a proxy for snowmelt. We derived this indicator from measurements on the sampling day and the previous days, varying from 1 to 30 days. Then, we excluded snow depth losses up to 5 cm to remove noisy data. We also derived the snow presence from these data when snow depth was exceeding 5 cm.

The temporal sensitivities of agreement between nivo-meteorological indicators and hydrochemical signatures were expressed as Spearman rank correlation coefficients ($p < 0.05$) and represented a measure to obtain the most relevant nivo-meteorological indicators to be considered for further analysis in this study.

In order to understand the link among water sources and their hydrochemical composition, a principle component analysis (PCA), using data centred to null and scaled to variance one (R core team, 2016), was performed. Data below detection limit were excluded from the analysis.

To assess the dampening effect of meltwater on stream water chemistry during baseflow conditions and the melting period, the variability coefficient (VC) was calculated following Sprenger et al. (2016) (Eq. 1):

246 $VC = SD_{baseflow}/SD_{melting}$ (1)

247 where $SD_{baseflow}$ is the standard deviation of stream EC sampled during baseflow conditions in
248 winter at a given location and $SD_{melting}$ is the standard deviation of stream EC at the same
249 locations during the melting period in summer.

250 We applied a two-component mixing model based on EC and δ^2H data to separate the runoff
251 contributions originating from the Sulden and Trafoi sub-catchment at each sampling moment
252 during monthly sampling (Sklash and Farvolden, 1979), following Eq. (2) and Eq. (3):

253 $Q_{S1} = Q_{S2} + Q_{T1}$ (2)

254 $P_{T1} = (C_{S2} - C_{S1})/(C_{S2} - C_{T1})$ (3)

255 where P is the runoff proportion, C is the EC or isotopic composition in ^2H measured at the
256 locations S1 (outlet), S2 (sampling location in the Sulden sub-catchment upstream the
257 confluence with Trafoi River), and T1 (sampling location in the Trafoi sub-catchment
258 upstream the confluence with Sulden River, see Fig. 1). The uncertainty in this calculation
259 was expressed as Gaussian error propagation using the instrumental precision of the
260 conductivity meter (0.1 µS cm^{-1}) and sample standard deviation from the laser spectroscope,
261 following Genereux (1998). Furthermore, statistical analysis was performed to test the
262 variance of hydrochemical data by means of a t-test (if data followed normal distribution) or a
263 nonparametric Mann-Whitney Rank Sum test (in case of not-normally distributed data).

264 # 3 Results

265 ## 3.1 Origin of water sources

266 Element concentrations of stream and rock glacier spring water are presented in Table S1 and
267 S2. It is worth highlighting that heavy metal concentrations (such as Al, V, Cr, Ni, Zn, Cd,
268 Pb) showed the highest concentrations during intense melting in July 2015 at all six locations
269 (partly exceeding concentration thresholds for drinking water (see European Union Drinking
270 Water Regulations 2014). Element concentrations were clearly higher at the most upstream
271 sampling locations. Relatively low variability coefficients (VC < 0.3) for these elements
272 confirmed that larger variations of concentrations occurred during the melting period and not
273 during baseflow conditions. Interestingly, the highest heavy metal concentrations (such as
274 Mn, Fe, Cu, Pb) of rock glacier springs SPR2 – 4 delayed the heavy metal concentration peak
275 in the stream by about two months.

In contrast, other element concentrations (such as As, Sr, K, Sb) generally revealed higher concentrations during baseflow conditions and lower concentrations during the melting period. This observation was corroborated by relatively high variability coefficients for As (VC: 2 – 2.9) and Sb (VC: 2 – 2.2) at S1, S2, and T1. For example, while highest Sr concentrations were measured at S6, As was highest at the downstream locations T1, S2, and S1. Regarding the rock glacier springs, their hydrochemistry showed a gradual decrease in As and Sr concentration from July to September 2015. The observed geochemical patterns are confirmed by PCA results (Fig. 2) and the correlation matrix (Fig. 3), revealing that geochemical dynamics are driven by temporal (PC1) and spatial controls (PC2) and a typical clustering of elements, respectively. PC1 showed high loadings for heavy metal concentrations (such as Al, V, Cr, Ni, Zn, Cd, Pb), supporting the clear temporal dependency for the entire catchment (baseflow conditions vs. melting period) (Fig. 2a). PC2 was instead mostly characterized by high loadings of δ^2H and $\delta^{18}O$ in the Trafoi sub-catchment (i.e. T1 and TT2) and geochemical characteristics (EC, Ca, K, As and Sr) from the upstream region of the Sulden River and rock glacier spring water (i.e. S6 and SSPR2-4, respectively). Overall, temporal and spatial controls explained a variance of about 53 %.

3.2 Temporal and spatial tracer variability in the sub-catchments

The temporal and spatial variability of EC in the Sulden and Trafoi River along the different sections, their tributaries, and springs is illustrated in Fig. 4. During baseflow conditions, from late autumn to early spring prior to the onset of the melting period in May/June, water enriched in solutes had an important impact on stream hydrochemistry as stream and tributary locations showed the most increased conductivity, ranging from 132.5 to 927 µS cm^{-1} in January to March 2015. During the same period, isotopic composition was slightly more enriched (δ^2H -96.7 – 102.5 ‰) and spatially more homogeneous among the stream (δ^2H: -96.7 – 102.5 ‰), tributaries (δ^2H: -96.5 – 109.8 ‰), and springs (δ^2H: -96.5 – 104 ‰) than in the summer months. In contrast, during the melting period, water from all sites in both sub-catchments became diluted due to different inputs of meltwater (Fig. 4a, b), while water was most depleted during snowmelt dominated periods (e.g., mid-June 2014 and end of June 2015) and less depleted during glacier melt dominated periods (e.g., mid to end of July 2014 and 2015) (Fig. 4c and 4d). Rainfall became a dominant runoff component during intense

storm events. For instance, on 24 September 2015, a storm of 35 mm d^{-1} resulted in the strongest isotopic enrichment of this study, which is visible in Fig. 4c at T3 and TT2 (δ^2H -86.9 ‰; $\delta^{18}O$: -12.4 ‰).

Hereinafter, the hydrochemistry of the Sulden and Trafoi sub-catchment is analyzed in terms of hydrochemical patterns of the main stream, tributaries, springs, and runoff contributions at the most downstream sampling location above the confluence. At T1 and S2, hydrochemistry was statistically different in its isotopic composition (Mann-Whitney Rank Sum Test: $p < 0.001$) but not in EC (Mann-Whitney Rank Sum Test: $p = 0.835$). Runoff originating from Trafoi and derived from the two-component HS, contributed to the outlet by about 36 % (±0.004) to 58 % (±0.003) when using EC and ranged from 29 % (±0.09) to 83 % (±0.15) when using δ^2H. These streamflow contributions expressed as specific discharge from Trafoi sub-catchment (and Sulden sub-catchment) were 20.6 (37.1) and 16.2 (12) l s^{-1} km^{-2} for EC and 50.4 (121.9) and 12.2 (2.6) l s^{-1} km^{-2} for δ^2H, respectively. Therefore, with respect to the temporal variability of the sub-catchment contributions, runoff at the outlet was sustained more strongly by the Trafoi River during non-melting periods while the runoff from the Sulden sub-catchment dominated during the melting period.

By the aid of both tracers, catchment specific hydrochemical characteristics such as contrasting EC gradients along the stream were revealed (Fig. 4 and Fig. 5). EC in the Trafoi River showed linearly increasing EC with increasing catchment area (from T3 to T1) during baseflow and melting periods (EC enrichment gradient).

In contrast, the Sulden River revealed relatively high EC (926 µS cm^{-1}) at the highest upstream location (S6) and relatively low EC (393 µS cm^{-1}) upstream the confluence with the Trafoi River (S2) during baseflow conditions in January to March 2015. The exponential decrease in EC (EC dilution gradient) during this period of time was strongly linked to the catchment area ($R^2 = 0.85$). Surprisingly, the EC dilution along the Sulden River was still persistent during melting periods but highly reduced. In this context, it is also interesting to compare the EC variability (expressed as VC) along Trafoi and Sulden River during baseflow conditions and melting periods (Table 4). For both streams, VC increased with decreasing distance to the confluence (Trafoi River) and the outlet (Sulden River), and thus representing an increase in catchment size. The highest EC variability among all stream sampling locations is given by the lowest VC, which was calculated for S6. This location represents the closest

one to the glacier terminus and showed a pronounced contrast of EC during baseflow conditions and melting periods (see Fig. 4 and Fig. 5).

Regarding the hydrochemical characterisation of the tributaries in both sub-catchments (Fig. 4), Sulden tributaries were characterised by a relatively low EC variability (68.2 – 192.3 µS cm^{-1}) and more negative isotopic values (δ^2H: -100.8 – 114.5 ‰) compared to the higher variability in hydrochemistry of the Sulden River. In contrast, the tracer patterns of Trafoi tributaries were generally consistent with the ones from the stream. Generally, also spring water at TSPR1, TSPR2, and SSPR1 followed these patterns during baseflow and melting periods in a less pronounced way, possibly highlighting the impact of infiltrating snowmelt into the ground. Comparing both springs sampled in the Trafoi sub-catchment indicated that spring waters were statistically different only when using EC (Mann-Whitney Rank Sum Test: $p = 0.039$). While TSPR1 hydrochemistry was slightly more constant, the one of TSPR2 was more variable from June to August 2015 (Fig. 4).

3.3 Meteorological controls on hydrometric and hydrochemical stream responses

To identify the effect of meteorological controls at high elevations on the hydrometric and hydrochemical stream response at the outlet, we first present the relationship between meteorological parameters against snow depth differences (Fig. 6). Then, we show snow depth differences compared with discharge, EC and isotopic data (Fig. 7).

Among the nivo-meteorological indicators listed in Table 3, daily maximum air temperature T_{max} and daily maximum global solar radiation G_{max} were the most important drivers to control snowmelt (expressed as snow depth differences) at high elevations (Fig. 6). While moderate snow depth losses by up to 30 cm occurred during days with T_{max} between 0 and 5°C, higher snow depths losses (up to 80 cm) were associated with warmer days, when T_{max} ranged between 5 and 12.5 °C at AWS Madritsch.

With respect to G_{max}, only small snow depth losses of up to 10 cm and small variability were present when G_{max} ranged from 600 to 1000 W m^{-2}. As soon as the daily maximum of 1000 W m^{-2} was exceeded, snow depth losses could reach a maximum of up to 80 cm. When exceeding these T_{max} and G_{max} thresholds, the variability of snow depth losses remarkably increased and increased with the time scale of the observation period.

As a consequence, high elevation snowmelt played an important role in explaining both the hydrometric and hydrochemical response at the outlet Stilfserbrücke (Fig. 7). During the

snowmelt period, discharge at the outlet clearly increased with increasing snowmelt due to snow depth losses at high elevation. For example, median discharges of 6.25 and 7.5 $m^3 s^{-1}$ resulted from snow depth losses of 50 and 75 cm while discharges higher than 20 $m^3 s^{-1}$ occurred when snow depth losses were higher than 100 cm during the previous days.

Moreover, the increasing amount of snowmelt resulted in decreasing EC and lower $\delta^{18}O$. While median EC of about 250 µS cm^{-1} was still relatively high after snow depth losses between 50 and 75 cm occurred, highest losses induced a drop in EC of about 50 µS cm^{-1}. With respect to the same snow depth losses, median stream water $\delta^{18}O$ reached -13.8 ‰ and ranged between -14.1 and -14.3 ‰, respectively. However, due to higher variability of $\delta^{18}O$, the effect of snowmelt on the isotopic composition was less clear than the dilution effect on EC.

3.4 Temporal variability at the catchment outlet

The temporal variability of the hydrochemical variables observed at the catchment outlet and of the meteorological drivers is illustrated in Fig. 8. Controlled by increasing radiation inputs and air temperatures above about 5°C in early summer (Fig. 6, Fig. 7, Fig. 8a and 8b), first snowmelt-induced runoff peaks in the Sulden River were characterised by EC of about 200 µS cm^{-1} and a depleted isotopic signature of about -14.6 ‰ in $\delta^{18}O$. These runoff peaks reached about 20 $m^3 s^{-1}$, starting from a winter baseflow of about 1.8 $m^3 s^{-1}$ (Fig. 8c and 8e). In comparison, the average snowmelt EC was 28 µS cm^{-1} and -14.84 ‰ in $\delta^{18}O$. Later in the summer, glacier melt-induced runoff peaks reached about 13 – 18 $m^3 s^{-1}$, characterised by relatively low EC (about 235 µS cm^{-1}) and isotopically more enriched stream water ($\delta^{18}O$: about -13.3 ‰). In fact, glacier melt showed an average EC of 36.1 µS cm^{-1} and average of 13.51 ‰ in $\delta^{18}O$. The highest discharge measured during the analysed period (81 $m^3 s^{-1}$ on 13 August 2014) was caused by a storm event, characterized by about 31 mm of precipitation falling over 3 hours at AWS Madritsch. Unfortunately, isotopic data for this event were not available due to a technical problem with the automatic sampler.

Water turbidity was highly variable at the outlet, and mirrored the discharge fluctuations induced by meltwater or storm events. Winter low flows were characterised by very low turbidity (< 10 NTU, corresponding to less than 6 mg l^{-1}). In summer, turbidity ranged between 20 and up to 1200 NTU during cold spells and melt events combined with storms,

respectively. However, the maximum value recorded was 1904 NTU reached after several storm events of different precipitation amounts (17 mm, 50 mm, and 9 mm) on 12, 13, and 14 August 2014, respectively. Unfortunately, the turbidimeter did not work properly after the August 2014 flood peak, in mid-July 2015 and beginning of October 2015.

Furthermore, the interannual variability of meteorological conditions with respect to the occurrence of days exceeding 6.5 or 15 °C threshold of daily maximum air temperature, storm events and snow cover characterized the contrasting years 2014 and 2015. (Fig.8 and Table 1). While about 250 cm of maximal snowpack depth in 2014 lasted until mid-July, only about 100 cm were measured one year after with complete disappearance of snow one month earlier. In 2015, several periods of remarkable warm days occurred reaching more than 15°C at 2825 m a.s.l. and led to a catchment entirely under melting conditions (freezing level above 5000 m a.s.l., assuming the mean atmospheric lapse rate of 6.5 °C km^{-1} (Kaser et al., 2010)). In contrast, days with daily maximum air temperature higher than 6.5 °C (freezing level at the highest peak in the study area) and 15 °C (about 8.1°C at the highest peak) in 2014 were less than days with similar conditions in 2015 or did not occur at all, respectively. Intense storms of up to 50 mm d^{-1} were registered three times in 2014 and only once in 2015. Despite a relatively similar hydrograph with same discharge magnitudes during melt-induced runoff events in both years, EC and $\delta^{18}O$ clearly characterized snowmelt and glacier melt-induced runoff events in 2014. However, a characteristic period of depleted or enriched isotopic signature was lacking in 2015 so that snowmelt and glacier melt-induced runoff events were graphically more difficult to distinguish.

The daily variations in air temperature, discharge, turbidity, and EC showed marked differences in the peak timing. Daily maximum air temperature generally occurred between 12:00 and 15:00, resulting in discharge peaks at about 22:00 to 1:00 in early summer and at about 16:00 to 19:00 during late summer. Turbidity peaks were measured at 22:00 to 23:00 in May to June and distinctively earlier at 16:00 to 19:00 in July and August. In contrast, EC maximum occurred shortly after the discharge peak between 00:00 to 1:00 in early summer and at 11:00 to 15:00, clearly anticipating the discharge peaks.

It is interesting to highlight a complex hydrochemical dynamics during the baseflow period in November 2015, which was interrupted only by a precipitation event on 28 and 29 October 2015. This event was characterized by more liquid (12.9 mm) than solid precipitation (6.6 mm) falling on a snowpack of about 10 cm (at 2825 m a.s.l.). While stream discharge showed

a typical receding hydrograph confirmed by EC being close to the background value of about 350 µS cm^{-1}, $\delta^{18}O$ indicated a gradual isotopic depletion indicating the occurrence of isotopically depleted water (e.g., snowmelt) in the stream. Also turbidity slightly increased from 4.1 to 8.3 NTU during both days.

To better characterize the temporal dynamics of hydrochemical variables, Fig. 9 shows the different relationships of discharge, EC, $\delta^{18}O$, and turbidity grouped for different months. In general, high turbidity was linearly correlated with discharge, and showed a monthly trend (Fig. 9a). This behaviour can be explained by generally higher discharges during melting periods (June, July, and August) and lower ones during baseflow conditions. Discharge and EC exhibited a relationship characterised by a hysteretic pattern at the monthly scale (Fig. 9b), which was associated with the monthly increasing contribution of meltwater with lower EC during melting periods contrasting with dominant groundwater contributions and higher EC during baseflow conditions.

During these periods, $\delta^{18}O$ of stream water was mainly controlled by the dominant runoff components (i.e., snowmelt and glacier melt in early summer and mid- to late summer, respectively) rather than the amount of discharge (Fig. 9c). Similarly, the relationship between $\delta^{18}O$ and EC was driven by the discharge variability resulting in a specific range of EC values for each month and by the meltwater component generally dominant during that period (Fig. 9d). As $\delta^{18}O$ was dependent on the dominant runoff components and less on the amount of discharge, turbidity showed no clear relationship with the isotopic composition (Fig. 9e). In contrast, EC and turbidity were controlled by monthly discharge variations so that both variables followed the monthly trend, revealing a linear relationship (Fig. 9f).

Finally, we evaluated the hysteretic pattern of discharge and EC in more detail by comparing it against T_{max}, G_{max} and the snow presence (Fig. 10). While T_{max} at high elevation ranged between 0 and 5 °C and G_{max} already exceeded 1000 W m^{-2} during early summer, increasing discharge with decreasing EC was observed at the outlet. This pattern progressed further as more snowmelt was available due to T_{max} increasing to 5 to 10 °C and high G_{max}. Interestingly, highest discharges with lowest EC occurred during days with G_{max} > 1300 W m^{-2} but not during the warmest days when snow cover at high elevation was scattered. Thus, runoff events during this period of time were clearly snowmelt- and glacier melt-induced, also because only one storm event of P_{1d} = 12.2 mm was measured. In late summer and autumn,

discharges started to fall while EC increased during snow-free days with decreasing T_{max} but still high G_{max}. As soon as T_{max} was below 5 °C, discharges dropped below 10 $m^3 s^{-1}$ and EC rose above 250 µS cm^{-1}, characterizing the initial phase of baseflow conditions in the Sulden River.

4 Discussion

4.1 Geological controls on the stream hydrochemistry

Hydrochemical dynamics were driven by a pronounced release of heavy metals (such as Al, V, Cr, Ni, Zn, Cd, Pb) shown for the entire catchment and, in contrast, by a specific release of As and Sr in the upper and lower Sulden sub-catchment (Fig. 2). Yet, as the explained variance was only at about 53 %, further controls may be present. In this context, PC3 explained 11.8% of additional variance and may characterize the hydrochemistry of surface and subsurface flows resulting from different residence times within the different soils and rocks.

With respect to PC1, several sources of heavy metals could be addressed: these elements may be released by rock weathering on freshly-exposed mineral surfaces and sulphide oxidation, typically produced in metamorphic environments (Nordstrom et al., 2011). Proglacial stream hydrochemistry may also strongly depend on the seasonal evolution of the subglacial drainage system that contributes to the release of specific elements (Brown and Fuge, 1998). In this context, rock glacier thawing may play an important role for the release of Ni (Thies et al., 2007; Mair et al., 2011; Krainer et al., 2015) and Al and Mn (Thies et al., 2013). However, high Ni concentrations were not observed in this study. Moreover, high heavy metal concentrations were measured during the melting period in mid-summer, which would be generally too early to derive from permafrost thawing (Williams et al., 2006; Krainer et al., 2015). Also bedrock weathering as major origin probably needs to be excluded because low concentrations of heavy metals occurred in winter when the hydrological connectivity at higher elevations was still present (according to running stream water at the most upstream locations).

It is therefore more likely that heavy metals derive from meltwater itself, as the spatial and temporal dynamics indicated. The element release is strongly coupled with melting and infiltration processes, when hydrological connectivity within the catchment is expected to be

highest during the snowmelt period. To support this explanation, supplementary element analysis of selected snowmelt (n = 2) and glacier melt (n = 2) samples of this study were conducted. Although these samples did not contain high concentrations of Cd, Ni, and Pb (average concentration: 24.5, 10.2, and 9.6 µS cm^{-1}, respectively), snowmelt in contact with the soil surface was more enriched in such elements (150, 191, and 15 µS cm^{-1}, respectively) than dripping snowmelt. Moreover, in a previous study in the neighbouring Matsch/Mazia Valley in 2015, snowmelt and ice melt samples were strongly controlled by high Al, Co, Cd, Ni, Pb and Zn concentrations (Engel et al., 2017). As shown for 21 sites in the Eastern Italian Alps (Veneto and Trentino-South Tyrol region), hydrochemistry of the snowpack can largely be affected by heavy metals originating from atmospheric deposition from traffic and industry (such as V, Sb, Zn, Cd, Mo, and Pb) (Gabrielli et al., 2006). Likely, orographically induced winds and turbulences arising in the Alpine valleys may often lead to transport and mixing of trace elements during winter. Studies from other regions, such as Western Siberia Lowland and the Tibetan Plateau, agree on the anthropogenic origin of these metals (Shevchenko et al., 2016 and Guo et al., 2017, respectively).

In contrast, a clear geological source can be attributed to the origin of As and Sr, indicating a bedrock-specific geochemical signatures. In the lower Sulden catchment (at locations S1, S2, and T1), As could mainly originate from As-containing bedrocks. As-rich lenses are present in the cataclastic carbonatic rocks (realgar bearing) and in the mineralized, arsenopyrite bearing bands of quartzphyllites, micaschists and paragneisses of the crystalline basement. Different outcrops and several historical mining sites are known and described in the literature (Mair, 1996, Mair et al., 2002, 2009; Stingl and Mair, 2005). In the upper Sulden catchment, the presence of As is supported by the hydrochemistry of rock glacier outflows in the Zay sub-catchment (corresponding to the drainage area of ST2; Engel et al., 2018) but was not reported in other studies (Thies et al., 2007; Mair et al., 2011; Krainer et al., 2015; Thies et al., 2013). Also high-elevation spring waters in the Matsch Valley corroborated that As and Sr concentrations may originate from paragneisses and micaschists (Engel et al., 2017). However, the gradual decrease in As and Sr concentrations from rock glacier springs clearly disagrees with the observations from other studies that rock glacier thawing in late summer leads to increasing element releases (Williams et al., 2006; Thies et al., 2007; Krainer et al., 2015; Nickus et al., 2015). We suggest a controlling mechanism as follows: As and Sr originate from the Quarzphyllite rocks, that form the bedrock of the rock glaciers (see

Andreatta, 1952; Montrasio et al., 2012). Weathering and former subglacial abrasion facilitate this release (Brown, 2002). As- and Sr-rich waters may form during winter when few quantities of water percolate in bedrock faults and then are released due to meltwater infiltration during summer (V. Mair, personal communication, 2018). As a clear delayed response of heavy metal concentrations in rock glacier outflow was revealed, the infiltration and outflow processes along flow paths in the bedrock near the rock glaciers may take up to two months to hydrochemically respond to snowmelt contamination (Hood and Hayashi, 2015).

As a consequence, a clear hydrochemical signature of permafrost thawing is difficult to find and results may lack the transferability to other catchments as not all rock glaciers contain specific elements to trace (Colombo et al., 2017). In this context, as precipitation and snowmelt affect the water budget of rock glaciers (Krainer and Mostler, 2002; Krainer et al., 2007), potential impacts of atmospheric inputs on rock glacier hydrochemistry could be assumed and would deserve more attention in future (Colombo et al., 2017).

Furthermore, export of elements in fluvial systems is complex and may strongly be affected by the pH (Nickus et al., 2015) or interaction with solids in suspension (Brown et al., 1996), which could not be addressed in this study. Further insights on catchment processes might be gained considering also element analysis of the solid fraction, to investigate whether water and suspended sediment share the same provenance.

4.2 The role of nivo-meteorological conditions

Superimposing the impact of the geological origin, melting processes were controlled by meteorological conditions, affecting stream hydrochemistry during summer, as shown by isotope dynamics (Fig. 4 and 8) and hydrochemical relationships (Fig. 9). It is well known that snowmelt is mainly driven by radiation and temperature. Generally, radiation is the main energy source driving melt processes in glacierized catchments of different climates (Sicart et al., 2008; Vincent and Six (2013) and may integrate the effect of cloud coverage (Anslow et al., 2008). Moreover, a high correlation between snow or glacier melt and maximum air temperature exists (U.S. Army Corps of Engineers 1956; Braithwaite 1981), thus controlling daily meltwater contributions to streamflow (Mutzner et al., 2015; Engel et al., 2016). T_{max} is widely used for characterizing snow transformation processes such as the decay of snow albedo and snow metamorphism (e.g., Ragettli and Pellicciotti, 2012).

In this study, we show that T_{max} of about 5 °C and G_{max} of about 1000 W m^{-2} may represent important meteorological thresholds to trigger pronounced snow depth losses and thus snowmelt in the study area and other high-elevation catchments. In agreement with our findings, Ragettli and Pellicciotti (2012) used the same 5 °C threshold temperature for melt onset (as shown in Fig. 6a and Fig. 8).

Of course, further nivo-meteorological indicators such as the extent of snow cover (Singh et al., 2005), vapour pressure, net radiation, and wind (Zuzel and Cox, 1975) or turbulent heat fluxes and long-wave radiation (Sicart et al., 2006) may exist but were not included in the present study due to the lack of observations.

Moreover, with respect to spatial representativeness, T_{max} and G_{max} represent point-scale data from the only high-elevation AWS of this catchment, providing the nivo-meteorological indicators needed for this study. However, not only elevation controls snowmelt but also spatial variability of other factors such as aspect, slope, and microtopography (e.g., Anderton et al. 2002; Grünewald et al. 2010; Lopez-Moreno et al. 2013), which could not be addressed here. These site characteristics usually lead to different melt rates and thus affect the isotopic snowmelt signature (Taylor et al. 2001; Dietermann and Weiler, 2013) and the hydrometric response in the main channel such as the timing of the discharge peak (Lundquist and Dettinger, 2005).

The temporal sensitivity analysis and the relatively large variability related to snow depth losses (Fig. 6 and Fig. 7) are generally difficult to compare due to the lack of suitable studies. Moreover, we considered ΔSD of up to 5cm as noisy data, but we did not discard data when strong winds occurred, likely resulting in pronounced blowing snow. In addition, decreasing snow depth may be the result of undergoing snow compaction, not related to the release of melt water from the snowpack. Therefore, the use of snow depth losses as proxy for snowmelt has to be considered with care.

The contrasting variabilities of discharge, EC, and $\delta^{18}O$ with respect to the observed time scale (Fig. 7) may also result from different flow paths and storages in the catchment, such as the snowpack itself as short-term storage for meltwater ranging from few hours to few days (Coléou and Lesaffre, 1998). Slower and quicker flow paths within glacial till, talus, moraines, and shallow vs. deeper groundwater compartments could indicate intermediate and longer (14 days) meltwater response (Brown et al., 2006; Roy and Hayashi, 2009; McClymont et al., 2010; Fischer et al., 2015; Weiler et al., 2017).

4.3 Implications for streamflow and hydrochemistry dynamics

Tracer dynamics of EC and stable isotopes associated with monthly discharge variations generally followed the conceptual model of the seasonal evolution of streamflow contributions (for example, isotopic depletion and low EC during snowmelt period in June, less isotopic depletion and low EC during glacier melt period), as described for catchments with a glacierized area of 17 % (Penna et al. 2017a) and 30 % (Schmieder et al. 2017). However, isotopic dynamics were less pronounced compared to these studies, likely resulting from the impact of relative meltwater contribution related to different catchment sizes, the proportion of glacierized area (Baraer et al., 2015) or the sampling year

In addition, hydrometric and geochemical dynamics analysed in this study were controlled by an interplay of meteorological conditions, the heterogeneity of geology, and topography. Such an interplay is highlighted by EC dynamics further controlled by the contributing catchment area (i.e., EC gradients along the Sulden and Trafoi River) (Wolock et al., 1997; Peralta-Tapia et al. 2015; Wu 2018). As EC was highly correlated to Ca concentration (Spearman rank correlation: 0.6, $p < 0.05$; see Fig. 3), EC dynamics were determined by the spatial distribution of different geology. For example, as dolomitic rocks are present almost within the entire Trafoi sub-catchment, meltwater following the hydraulic gradient can likely become more enriched in solutes with longer flow pathways and increasing storage capability related to the catchment size (Fig. 5). As consequence, the EC enrichment gradient could persist during both the melting period and baseflow conditions in the presence of homogenous geology. Therefore, topography may become a more important control on spatial stream water variability than the geological substratum. In the Sulden sub-catchment, however, dolomitic rocks are only present in the upper part of the catchment while metamorphic rocks mostly prevail. This leads to a pronounced dilution during baseflow conditions of Ca-rich waters with increasing catchment area or in other words, increasing distance from the source area (Fig. 5). This implies that meltwater contributions to the stream homogenize the effect of geographic origin on different water sources, having the highest impact in vicinity of the meltwater source (see Table 4).

The additional effect of topographical characteristics is underlined by the findings that the Sulden River hydrochemistry at S2 was significantly more depleted in δ^2H and $\delta^{18}O$ than T1 hydrochemistry. Compared with the Sulden sub-catchment, the Trafoi sub-catchment has a

slightly higher proportion of glacier extent but, more importantly, has a clearly smaller catchment area within the elevation bands of 1800 to 3200 m a.s.l. (i.e., 40.2 km² for the Trafoi and 66.5 km² for the Sulden sub-catchment). In this elevation range, the sub-catchments of major tributaries ST1, ST2, and ST3 are situated, which deliver large snowmelt contributions to the Sulden River (Fig. 4 and Fig. 5).

Meteorological conditions, geology and topography explain specific hydrometric and hydrochemical relationships at the catchment outlet. For example, the hysteretic relationship between discharge and EC (Fig. 8b) corresponds well with the hysteresis observed in the nearby Saldur and Alta Val de La Mare catchment (Engel et al., 2016; Zuecco et al. 2016), although these studies focused on the runoff event scale. The initial phase of this hysteresis in early summer was clearly snowmelt-induced with snowmelt likely originating from lower elevations as T_{max} at high elevation was still relatively low (0 – 5°C). The further development of the hysteresis is then linked to the progressing snowmelt contribution towards higher elevations. In contrast, the phase of hysteresis in late summer to early autumn is determined by glacier melt and its decreasing contributions when low T_{max} and G_{max} indicate the lack of available energy for melting.

Moreover, this relationship helps to identify the conditions with maximum discharge and EC: during baseflow conditions, the Sulden River showed highest EC of about 350 µS cm^{-1} seemingly to be bound to only about 3 m^3 s^{-1} whereas the maximum dilution effect occurred during a storm on 29 June 2014 (55 mm of precipitation at AWS Madritsch) with 29.3 m^3 s^{-1} of discharge resulting in only 209 µScm^{-1}. However, these observations are based on daily data sampled at 23:00, likely not capturing the entire hydrochemical variability inherent of the Sulden catchment. As shown in Fig. 5 and Fig. 7, much higher discharges and thus even lower EC could be reached along the Sulden River and inversely, which was potentially limited by the specific geological setting of the study area.

As more extreme weather conditions (such as heat waves, less solid winter precipitation) are expected in future (Beniston, 2003; Viviroli et al., 2011; Beniston and Stoffel 2014), glacierized catchments may exhibit more pronounced hydrochemical responses such as shifted or broader ranges of hydrochemical relationships (Kumar et al., 2018) and increased heavy metal concentrations both during melting periods and baseflow conditions. However, identifying these relationships with changing meteorological conditions would deserve more attention and is strongly limited by our current understanding of underlying hydrological

processes (Schaefli et al., 2007). In a changing cryosphere, more complex processes such as non-stationarity processes may emerge under changing climate, which was found to be a major cause of non-stationarity (Milly et al., 2008). In this context, explaining apparently ambiguous processes as the one we observed during the baseflow period in November 2015 (Fig. 8) will deserve further attention.

Finally, our results underline that long-term controls such as geology and topography govern hydrochemical spatial responses (such as bedrock-specific geochemical signatures, EC gradients, and relative snowmelt contribution). In contrast, short-term controls such as daily maximum solar radiation, air temperature, and snow depth differences drive short-term responses (such as discharge variability and EC dilution). Both statements are in general agreement with the findings of Heidbüchel et al. (2013). However, as the catchment response strongly depended on the melting period vs. baseflow conditions, controls at longer temporal scales interact as well. Thus, our findings suggest that glacierized catchments react in a much more complex way compared to non-glacierized catchments, and that catchment responses cannot be attributed to one specific scale, justified by either short-term or long-term controls alone.

In this context, the present study provides novel insights into geological, meteorological, and topographic controls of stream water hydrochemistry rarely addressed for glacierized catchments so far. Moreover, this study strongly capitalizes on an important dataset that combines nivo-meteorological indicators and different tracers (stable isotopes of water, EC, major, minor and trace elements). This aspect finally underlines the need for conducting multi-tracer studies in glacierized catchments with different geological complexity, in order to evaluate whether our findings (obtained in sedimentary and metamorphic substratum) are transferable to different geological settings.

4.4 Methodological limitation

The sampling approach combined a monthly spatial sampling with daily sampling at the outlet, which methodologically is in good agreement with other sampling approaches, accounting for increasing distance of sampling points to the glacier (Zhou et al., 2014; Baraer et al., 2015), intense spatial and temporal sampling (Penna et al., 2014; Fischer et al., 2015), synoptic sampling (Carey et al., 2013; Gordon et al., 2015), and different catchment structures such as nested catchments (Soulsby et al., 2006b). Sampling covered a variety of days with

typical snowmelt, glacier melt and baseflow conditions during 2014 and 2015, confirming the representativeness of tracer dynamics within two years with contrasting meteorological characteristics (Table 1). However, short-term catchment responses (such as storm-induced peak flows and related changes in hydrochemistry) were difficult to capture by this sampling approach, and would require a higher temporal sampling resolution. In this context, also the representativeness of the outlet sampling time with respect to the peak discharge time at that location may play an important role. In fact, the peak of hydrochemical response may not be synchronized with the hydrometric one and therefore may lead to stronger or weaker relationships.

Furthermore, two years of field data are probably not sufficient to capture all hydrological dynamics, hydrological catchment status and catchment responses to specific meteorological conditions. In this regards, long-term studies may have better chances in capturing the temporal variability of hydrochemical responses (Thies et al., 2007). Although time-, energy- and money-consuming, more complex and long sampling approaches should be developed to further unravel process understanding of glacierized catchments.

5 Conclusions

Our results highlight the complex hydrochemical responses of mountain glacierized catchments at different temporal and spatial scales controlled by meteorological conditions, topography and geological heterogeneity. To our knowledge, only few studies investigated the impact of controlling factors on stream water hydrochemistry by using nivo-meteorological indicators and multi-tracer data, which we recommend to establish as prerequisite for studies in other glacierized catchments.

The main results of this study can be summarized as follows:

- Hydrometric and geochemical dynamics were controlled by an interplay of meteorological conditions and the geological heterogeneity. The majority of the variance (PC1: 36.3 %) was explained by heavy metal concentrations (such as Al, V, Cr, Ni, Zn, Cd, Pb), associated with atmospheric deposition on the snowpack and release through snowmelt. Remaining variance (PC2: 16.3 %) resulted both from the presence of a bedrock-specific geochemical signature (As and Sr concentrations) and the role of snowmelt contribution.

- The isotopic composition of rock glacier outflow was relatively similar to the composition of glacier melt whereas high concentrations of As and Sr may more likely result from bedrock weathering. Therefore, as the underlying geology may prevails over a thawing permafrost characteristics, a specific hydrochemical signature of rock glacier springs was difficult to obtain.
- At the monthly scale for different sub-catchments (spatial scale: 0.05 – 130 km²), both $\delta^{18}O$ and EC revealed complex spatial and temporal dynamics such as contrasting EC gradients during baseflow conditions and melting periods.
- At the daily scale for the entire study area (spatial scale: 130 km²), we observed strong relationships of hydrochemical variables, with mainly discharge and EC exhibiting a strong monthly relationship. This was characterised by a hysteretic-like pattern, determined by highest EC and lowest discharge during baseflow conditions and maximum EC dilution due to highest discharge during a summer storm.
- Daily maximum air temperature T_{max} and daily maximum global solar radiation G_{max} were the most important drivers to control snowmelt at high elevation. T_{max} of about 5 °C and G_{max} of about 1000 W m^{-2} may represent meteorological thresholds to trigger pronounced snow depth losses and thus snowmelt in the study area. However, the use of snow depth losses as proxy for snowmelt has to be considered with care due to uncertainties related to blowing snow or snow compaction without meltwater outflow.

Finally, this study may support future classifications of glacierized catchments according to their hydrochemical response under different catchment conditions or the prediction of appropriate end-member signatures for tracer-based hydrograph separation being valid at longer time scales.

6 Data availability

Hydrometeorological data are available upon request at the Hydrographic Office of the Autonomous Province of Bozen-Bolzano. Tracer data used in this study are freely available by contacting the authors.

7 Acknowledgements

This research is part of the GLACIALRUN project and funded by the foundation of the Free University of Bozen-Bolzano and supported by the project "Parco Tecnologico - Tecnologie ambientali".

The authors thank Andrea Rücker, Ana Lucia, Alex Boninsegna, Raffaele Foffa, and Michiel Blok for their field assistance. Giulia Zuecco and Luisa Pianezzola are thanked for the isotopic analysis at TESAF, University of Padova and Christian Ceccon for the isotopic analysis in the laboratory of the Free University of Bozen-Bolzano. We also thank Giulio Voto at EcoResearch s.r.l. (Bozen/Bolzano) for the element analysis. We appreciate the helpful support for the geological interpretation by Volkmar Mair. We acknowledge the project AQUASED, whose instrumentation infrastructure we could use. Furthermore, we thank the Hydrographic Office and the Department of Hydraulic Engineering of the Autonomous Province of Bozen-Bolzano for providing meteorological and hydrometric data. We acknowledge the Forestry Commission Office Prat, the National Park Stilfser Joch / Passo Stelvio, and the Cable car Sulden GmbH for their logistical support and helpful advices.

8 References

Anderton, S., White, S. and Alvera, B.: Micro-scale spatial variability and the timing of snow melt runoff in a high mountain catchment, J. Hydrol., 268(1–4), 158–176, doi:10.1016/S0022-1694(02)00179-8, 2002.

Andreatta, C.: Polymetamorphose und Tektonik in der Ortlergruppe. - N. Jb. Mineral. Mh. Stuttgart, 1, 13–28, 1952.

Anslow, F. S., Hostetler, S., Bidlake, W. R. and Clark, P. U.: Distributed energy balance modeling of South Cascade Glacier, Washington and assessment of model uncertainty, J. Geophys. Res., 113(F02019), 1–18, doi:10.1029/2007JF000850, 2008.

Auer, A. H.: The rain versus snow threshold temperatures, Weatherwise, 27, 67, 1974.

Baraer, M., McKenzie, J., Mark, B. G., Gordon, R., Bury, J., Condom, T., Gomez, J., Knox, S. and Fortner, S. K.: Contribution of groundwater to the outflow from ungauged glacierized catchments: a multi-site study in the tropical Cordillera Blanca, Peru, Hydrol. Process., 29, 2561–2581, doi: 10.1002/hyp.10386, 2015.

Beniston, M.: Climatic change in mountain regions: a review of possible impacts; Clim. Change. 59, 5–31, doi: 10.1023/A: 1024458411589, 2003.

Beniston, M.: Mountain weather and climate: A general overview and a focus on climatic change in the Alps; Hydrobiologia, 562, 3–16, doi: 10.1007/s10750-005-1802-0, 2006.

Beniston, M., and Stoffel, M.: Assessing the impacts of climatic change on mountain water resources, Sci. Total Environ. 493, 1129–37, doi: 10.1016/j.scitotenv.2013.11.122, 2014.

Boeckli, L., Brenning, A., Gruber, S., and Noetzli, J.: A statistical approach to modelling permafrost distribution in the European Alps or similar mountain ranges, Cryosph., 6, 125–140, doi: 10.5194/tc-6-125-2012, 2012.

Braithwaite, R. J.: On glacier energy balance, ablation, and air temperature, J. Glaciol., 27, 381–391, 1981.

Brown, G. H.: Glacier meltwater hydrochemistry, Appl. Geochemistry, 17(7), 855–883, doi:10.1016/S0883-2927(01)00123-8, 2002.

785 Brown, G.H., and Fuge, R.: Trace element chemistry of glacial meltwaters in an Alpine
786 headwater catchment, Hydrol. Water Resour. Ecol. Headwaters, 2, 435–442, 1998.

787 Brown, G. H., Tranter, M., and Sharp, M.: Subglacial chemical erosion—seasonal variations
788 in solute provenance, Haut Glacier d'Arolla, Switzerland, Ann. Glaciol., 22, 25-31,
789 1996.

790 Brown, L.E., Hannah, D.M., Milner, A.M., Soulsby, C., Hodson, A.J., and Brewer, M.J.:
791 Water source dynamics in a glacierized alpine river basin (Taillon-Gabiétous, French
792 Pyrénées), Water Resour. Res., 42, doi: 10.1029/2005WR004268, 2006.

793 Carey, S. K., Boucher, J. L. and Duarte, C. M.: Inferring groundwater contributions and
794 pathways to streamflow during snowmelt over multiple years in a discontinuous
795 permafrost subarctic environment (Yukon, Canada), Hydrogeol. J., 21, 67–77, doi:
796 10.1007/s10040-012-0920-9, 2013.

797 Carey, S.K. and Quinton, W.L.: Evaluating runoff generation during summer using
798 hydrometric, stable isotope and hydrochemical methods in a discontinuous permafrost
799 alpine catchment, Hydrol. Process., 19, 95–114. doi:10.1002/hyp.5764, 2005.Carrillo,
800 G., Troch, P.A., Sivapalan, M., Wagener, T., Harman, C., Sawicz, K.: Catchment
801 classification: hydrological analysis of catchment behavior through process-based
802 modeling along a climate gradient, Hydrol. Earth Syst. Sci., 15, 3411–3430,
803 doi:10.5194/hess-15-3411-2011, 2011.

804 Carturan, L., Zuecco, G., Seppi, R., Zanoner, T., Borga, M., Carton, A. and Dalla Fontana, G.:
805 Catchment-Scale Permafrost Mapping using Spring Water Characteristics, Permafr.
806 Periglac. Process., 27(3), 253–270, doi:10.1002/ppp.1875, 2016.

807 Chiogna, G., Majone, B., Cano Paoli, K., Diamantini, E., Stella, E., Mallucci, S., Lencioni,
808 V., Zandonai, F. and Bellin, A.: A review of hydrological and chemical stressors in the
809 adige catchment and its ecological status, Sci. Total Environ. 540, 429–443,
810 doi:10.1016/j.scitotenv.2015.06.149, 2016.

811 Clark, I.D., Lauriol, B., Harwood, L., Marschner, M.: Groundwater contributions to discharge
812 in a permafrost setting, Big Fish River, N.W.T., Canada, Arct. Antarct. Alp. Res., 33,
813 62–69, 2001.

814 Coléou, C., and Lesaffre, B.: Irreducible water saturation in snow: experimental results in a
815 cold laboratory, Ann. Glaciol., 26, 64–68, 1998.

816 Colombo, N., Salerno, F., Gruber, S., Freppaz, M., Williams, M., Fratianni, S. and Giardino,
817 M.: Review: Impacts of permafrost degradation on inorganic chemistry of surface
818 fresh water, Glob. Planet. Change, 162, 69–83, doi:10.1016/j.gloplacha.2017.11.017,
819 2017.

820 Cook, S.J., and Swift, D.A.: Subglacial basins: Their origin and importance in glacial systems
821 and landscapes, Earth-Science Rev. 115, 332–372, doi:
822 10.1016/j.earscirev.2012.09.009, 2012.

823 Cortés, G., Vargas, X., McPhee, J.: Climatic sensitivity of streamflow timing in the
824 extratropical western Andes Cordillera, J. Hydrol., 405, 93–109, doi:
825 10.1016/j.jhydrol.2011.05.013, 2011.

826 Devito, K., Creed, I., Gan, T., Mendoza, C., Petrone, R., Silins, U., and Smerdon, B.: A
827 framework for broad-scale classification of hydrologic response units on the Boreal
828 Plain: Is topography the last thing to consider? Hydrol. Process., 19, 1705–1714,
829 doi:10.1002/hyp.5881, 2005.

830 Dietermann, N. and Weiler, M.: Spatial distribution of stable water isotopes in alpine snow
831 cover, Hydrol. Earth Syst. Sci., 17(7), 2657–2668, doi:10.5194/hess-17-2657-2013,
832 2013.

833 Dye, D.G.: Variability and trends in the annual snow-cover cycle in Northern Hemisphere
834 land areas, 1972-2000, Hydrol. Process., 16, 3065–3077, doi:10.1002/hyp.1089, 2002.

835 Engel, M., Penna, D., Bertoldi, G., Dell'Agnese, A., Soulsby, C., and Comiti, F.: Identifying
836 run-off contributions during melt-induced runoff events in a glacierized Alpine
837 catchment, Hydrol. Process., 30, 343–364, doi:10.1002/hyp.10577, 2016.

838 Engel, M., Penna, D., Tirler, W., and Comiti F.: Multi-Parameter-Analyse zur
839 Charakterisierung von Landschaftsmerkmalen innerhalb eines experimentellen
840 Messnetzes im Hochgebirge, In M. Casper et al. (Eds.): Den Wandel Messen –
841 Proceedings Tag der Hydrologie 2017, Forum für Hydrologie und
842 Wasserbewirtschaftung, Vol. 38, 293 – 299, 2017.

Engel, M., Brighenti S., Bruno MC., Tolotti M., Comiti F.: Multi-tracer approach for characterizing rock glacier outflow, 5th European Conference on Permafrost, Chamonix-Mont Blanc, 2018.

Epstein, S. and Mayeda, T.: Variation of $\delta^{18}O$ content in waters from natural sources, Geochim. Cosmochim. Ac., 4, 213–224, 1953.

Farvolden, R.N., Geological controls on ground-water storage and base flow, J. Hydrol., 1, 219–249, 1963.

Freyberg, J. Von, Studer, B. and Kirchner, J. W.: A lab in the field : high-frequency analysis of water quality and stable isotopes in stream water and precipitation, Hydrol. Earth Syst. Sci., 21, 1721–1739, doi:10.5194/hess-21-1721-2017, 2017.

Fischer, B. M. C., Rinderer, M., Schneider, P., Ewen, T. and Seibert, J.: Contributing sources to baseflow in pre-alpine headwaters using spatial snapshot sampling, Hydrol. Process., 29, 5321–5336, doi:10.1002/hyp.10529, 2015.

Gabrielli, P., Cozzi, G., Torcini, S., Cescon, P., Barbante, C.: Source and origin of atmospheric trace elements entrapped in winter snow of the Italian Eastern Alps, Atmos. Chem. Phys. Discuss., 6, 8781–8815, doi: 10.5194/acpd-6-8781-2006, 2006.

Galos, S.P., Klug, C., Prinz, R., Rieg, L., Sailer, R., Dinale, R., Kaser, G.: Recent glacier changes and related contribution potential to river discharge in the Vinschgau / Val Venosta, Italian Alps, Geogr. Fis. e Din. Quat., 38, 143–154, doi:10.4461/GFDQ.2015.38.13, 2015.

Gat, J. R. and Carmi, I.: Evolution of the isotopic composition of atmospheric waters in the Mediterranean Sea area, J. Geophys. Res., 75, 3039–3048, 1970.

Genereux, D.: Quantifying uncertainty in tracer-based hydrograph separations, Water Resour. Res., 34, 915–919, 1998.

Gordon, R. P., Lautz, L. K., McKenzie, J. M., Mark, B. G., Chavez, D. and Baraer, M.: Sources and pathways of stream generation in tropical proglacial valleys of the Cordillera Blanca, Peru, J. Hydrol., 522, 628–644, doi: 10.1016/j.jhydrol.2015.01.013 2015.

871 Gruber, S., Fleiner, R., Guegan, E., Panday, P., Schmid, M.O., Stumm, D., Wester, P., Zhang,
872 Y., and Zhao, L.: Review article: Inferring permafrost and permafrost thaw in the
873 mountains of the Hindu Kush Himalaya region, Cryosph, 11, 81–99, doi:10.5194/tc-
874 11-81-2017, 2017.

875 Grünewald, T., Schirmer, M., Mott, R. and Lehning, M.: Spatial and temporal variability of
876 snow depth and ablation rates in a small mountain catchment, Cryosph., 4(2), 215–
877 225, doi:10.5194/tc-4-215-2010, 2010.

878 Guo, B., Liu, Y., Zhang, F., Hou, J. and Zhang, H.: Heavy metals in the surface sediments of
879 lakes on the Tibetan Plateau , China, Environ. Sci. Pollut. Res., 25(4), 3695–3707, doi:
880 10.1007/s11356-017-0680-0, 2017.

881 Harris, C., Haeberli, W., Mühll, D.Vonder, and King, L.: Permafrost monitoring in the high
882 mountains of Europe: the PACE project in its global context, Permafr. Periglac.
883 Process., 12, 3–11, doi:10.1002/ppp, 2001.

884 Heidbüchel, I., Troch, P. A. and Lyon, S. W.: Separating physical and meteorological controls
885 of variable transit times in zero-order catchments, Water Resour. Res., 49(11), 7644–
886 7657, doi:10.1002/2012WR013149, 2013.

887 Hindshaw, R.S., Tipper, E.T., Reynolds, B.C., Lemarchand, E., Wiederhold, J.G.,
888 Magnusson, J., Bernasconi, S.M., Kretzschmar, R., and Bourdon, B.: Hydrological
889 control of stream water chemistry in a glacial catchment (Damma Glacier,
890 Switzerland), Chem. Geol., 285, 215–230, doi:10.1016/j.chemgeo.2011.04.012, 2011.

891 Hock, R.: A distributed temperature-index ice- and snowmelt model including potential direct
892 solar radiation, J. Glaciol., 45, 101–11, 1999.

893 Hodgkins, R.: Seasonal evolution of meltwater generation, storage and discharge at a non-
894 temperate glacier in Svalbard, Hydrol. Process., 15, 441–460, 10.1002/hyp.160, 2001.

895 Hood, J.L. and Hayashi, M.:. Characterization of snowmelt flux and groundwater storage in
896 an alpine headwater basin. J. Hydrol. 521, doi:10.1016/j.jhydrol.2014.12.041, 2015.

897 Humlum, O.: The geomorphic significance of rock glaciers: estimates of rock glacier
898 debris volumes and headwall recession rates in West Greenland, Geomorphology, 35,
899 41–67, 2000.

Immerzeel, W.W., van Beek, L.P.H., Konz, M., Shrestha, A. B., Bierkens, M.F.P.: Hydrological response to climate change in a glacierized catchment in the Himalayas, Clim. Change 110, 721–736, 2012.

International Atomic Energy Agency: IAEA/GNIP precipitation sampling guide V2.02 September 2014, International Atomic Energy Agency, Vienna, Austria, pp. 19, 2014.

IPCC, 2013. Climate Change 2013: The Physical Science Basis. Contribution of Working Group I to the Fifth Assessment Report of the Intergovernmental Panel on Climate Change. In: Stocker, T.F., Qin, D., Plattner, G.-K., Tignor, M., Allen, S.K., Boschung, J., Nauels, A., Xia, Y., Bex, V., Midgley, P.M., (Eds.), International Organization for Standardization Standard Atmosphere, ISO 2533, Cambridge University Press, Cambridge, United Kingdom and New York, NY, USA, 1535, pp. ISO, 1975.

Kaser, G., Grosshauser, M., and Marzeion, B.: Contribution potential of glaciers to water availability in different climate regimes, in: Proceedings of the National Academy of Sciences of the United States of America, 20223–20227, doi:10.1073/pnas.1008162107, 2010.

Katsuyama, M., Tani, M., and Nishimoto S.: Connection between streamwater mean residence time and bedrock groundwater recharge/discharge dynamics in weathered granite catchments, Hydrol. Process., 24, 2287–2299, doi:10.1002/hyp.7741, 2010.

Kirchner, J.W.: Catchments as simple dynamical systems: Catchment characterization, rainfall-runoff modeling, and doing hydrology backward, Water Resour. Res., 45, W02429, doi:10.1029/2008WR006912, 2009.

Kong, Y., and Pang, Z.: Evaluating the sensitivity of glacier rivers to climate change based on hydrograph separation of discharge, J. Hydrol. 434–435, 121–129, doi:10.1016/j.jhydrol.2012.02.029, 2012.

Krainer, K., and Mostler, W.: Hydrology of active rock glaciers: examples from the Austrian Alps, Arct. Antarct. Alp. Res., 34, 142–149, 2002.

Krainer, K., Mostler, W., and Spötl, C.: Discharge from active rock glaciers, Austrian Alps: a stable isotope approach, Austrian J. Earth Sc., 100, 102–112, 2007.

928 Krainer, K., Bressan, D., Dietre, B., Haas, J.N., Hajdas, I., Lang, K., Mair, V., Nickus, U.,
929 Reidl, D., Thies, H., and Tonidandel, D.: A 10,300-year-old permafrost core from the
930 active rock glacier Lazaun, southern Ötztal Alps (South Tyrol, northern Italy), Quat.
931 Res., 83, 324–335, doi:10.1016/j.yqres.2014.12.005, 2015.

932 Lamhonwah, D., Lafrenière, M.J., Lamoureux, S.F., and Wolfe, B.B.: Evaluating the
933 hydrological and hydrochemical responses of a High Arctic catchment during an
934 exceptionally warm summer, Hydrol. Process., 31, 2296–2313, doi:
935 10.1002/hyp.11191, 2017.

936 Lewis, T., Lafrenière, M.J., and Lamoureux, S.F.: Hydrochemical and sedimentary responses
937 of paired High Arctic watersheds to unusual climate and permafrost disturbance, Cape
938 Bounty, Melville Island, Canada, Hydrol. Process., 26, 2003–2018,
939 doi:10.1002/hyp.8335, 2012.

940 Liu, F., Williams, M.W., and Caine, N.: Source waters and flow paths in an alpine catchment,
941 Colorado Front Range, United States, Water Resour. Res., 40,
942 doi:10.1029/2004WR003076, 2004.

943 López-Moreno, J. I., Fassnacht, S. R., Heath, J. T., Musselman, K. N., Revuelto, J., Latron, J.,
944 Morán-Tejeda, E. and Jonas, T.: Small scale spatial variability of snow density and
945 depth over complex alpine terrain: Implications for estimating snow water equivalent,
946 Adv. Water Resour., 55, 40–52, doi:10.1016/j.advwatres.2012.08.010, 2013.

947 Lundquist, J. D. and Dettinger, M. D.: How snowpack heterogeneity affects diurnal
948 streamflow timing, Water Resour. Res., 41, 1–14, doi:10.1029/2004WR003649, 2005.

949 Mair, V.: Die Kupferbergbaue von Stilfs, Eyrs und Klausen, Der Stoansucher 10 (1), 38-44,
950 1996.

951 Mair, V., Lorenz, D., and Eschgfäller, M.: Mineralienwelt Südtirol. Verlag Tappeiner, Lana
952 (BZ), 215 S., 2009.

953 Mair, V., Müller, J.P., and Reisigl, H.: Leben an der Grenze. Konsortium Nationalpark
954 Stilfserjoch – Gemeinde Stilfs, Glurns (BZ), 120 S., 2002.

955 Mair, V., Nocker, C., and Tropper, P.: Das Ortler-Campo Kristallin in Südtirol, Mitt. Österr.
956 Mineral. Ges., 153, 219–240, 2007.

957 Mair, V., Zischg, A., Lang, K., Tonidandel, D., Krainer, K., Kellerer-Pirklbauer, A., Deline,
958 P., Schoeneich, P., Cremonese, E., Pogliotti, P., Gruber, S. and Böckli, L.: PermaNET
959 - Permafrost Long-term Monitoring Network. Synthesis report. INTERPRAEVENT
960 Journal series 1, Report 3. Klagenfurt, 2011.

961 Maurya, A.S., Shah, M., Deshpande, R.D., Bhardwaj, R.M., Prasad, A., and Gupta, S.K.:
962 Hydrograph separation and precipitation source identification using stable water
963 isotopes and conductivity: River Ganga at Himalayan foothills, Hydrol. Process., 25,
964 1521–1530, doi:10.1002/hyp.7912, 2011.

965 McClymont, A.F., Hayashi, M., Bentley, L.R., Muir, D., and Ernst, E.,: Groundwater flow
966 and storage within an alpine meadow-talus complex, Hydrol. Earth Syst. Sci., 14, 859–
967 872, doi:10.5194/hess-14-859-2010, 2010.

968 McGuire, K. J., McDonnell, J. J., Weiler, M., Kendall, C., McGlynn, B. L., Welker, J. M., and
969 Seibert, J.: The role of topography on catchment-scale water residence time. Water
970 Resour. Res., 41. doi:10.1029/2004WR003657, 2005.

971 Milly, P.C.D., Betancourt, J., Falkenmark, M., Hirsch, R.M., Kundzewicz, Z.W., Lettenmaier,
972 D.P., Stouffer, R.J.: Stationarity is dead—whither water management? Science, 319,
973 573–574, doi:10.1126/science.1151915, 2008.

974 Milner, A., Brown, L.E., and Hannah, D.M.: Hydroecological response of river systems to
975 shrinking glaciers, Hydrol. Process. 23, 62–77, doi:10.1002/hyp.7197 2009.

976 Montrasio, A. Berra, F., Cariboni, M., Ceriani, M., Deichmann, N., Ferliga, C., Gregnanin,
977 A., Guerra, S., Guglielmin, M., Jadoul, F., Lonhghin, M., Mair, V., Mazzoccola, D.,
978 Sciesa, E. & Zappone, A.: Note illustrative della Carta geologica d'Italia alla scala
979 1:50.000 Foglio 024 Bormio. ISPRA, Servizio Geologico D'Italia; System Cart, Roma
980 2012, 150 S., 2012.

981 Moore, R. D., Fleming, S. W., Menounos, B., Wheate, R., Fountain, A., Stahl, K., Holm, K.
982 and Jakob, M.: Glacier change in western North America: influences on hydrology,
983 geomorphic hazards and water quality, Hydrol. Process., 23, 42–61,
984 10.1002/hyp.7162, 2009.

985 Mutzner, R., Weijs, S. V., Tarolli, P., Calaf, M., Oldroyd, J., and Parlange, M.B.: Controls on
986 the diurnal streamflow cycles in two subbasins of an alpine headwater catchment,
987 Water Resour. Res., 51, 3403–3418, doi:10.1016/0022-1694(68)90080-2, 2015.

988 Natali, C., Bianchini, G., Marchina, C., and Knöller, K.: Geochemistry of the Adige River
989 water from the Eastern Alps to the Adriatic sea (Italy): Evidences for distinct
990 hydrological components and water-rock interactions. Environ. Sci. Pollut. R., 23,
991 11677-11694. doi:10.1007/s11356-016-6356-3, 2016.

992 Nickus U., Krainer K., Thies H. and Tolotti M.: Blockgletscherabflüsse am Äußeren
993 Hochebenkar –Hydrologie, Wasserchemie und Kieselalgen. In: Schallart N. &
994 Erschbamer B. (eds), Forschung am Blockgletscher, Methoden udn Ergebnisse. Alpine
995 Forschungstelle Obergurgl, Innsbruck University Press, Innsbruck (A), 4: 117-134.
996 ISBN 978-3-902936-58-5, 2015.

997 Nordstrom, D. K. Hydrogeochemical processes governing the origin, transport and fate of
998 major and trace elements from mine wastes and mineralized rock to surface waters,
999 Appl. Geochem., 26, 1777−1791, 2011.

1000 Onda, Y., Komatsu, Y., Tsujimura, M., and Fujihara, J. I.: The role of subsurface runoff
1001 through bedrock on storm flow generation, Hydrol. Processes, 15, 1693–1706,
1002 doi:10.1002/hyp.234, 2001.

1003 Penna, D., Stenni, B., Šanda, M., Wrede, S., Bogaard, T.A., Gobbi, A., Borga, M., Fischer,
1004 B.M.C., Bonazza, M., and Chárová, Z.: On the reproducibility and repeatability of
1005 laser absorption spectroscopy measurements for δ2H and δ18O isotopic analysis,
1006 Hydrol. Earth Syst. Sci., 14, 1551–1566, doi:10.5194/hess-14-1551-2010, 2010.

1007 Penna, D., Stenni, B., Šanda, M., Wrede, S., Bogaard, T.A., Michelini, M., Fischer, B.M.C.,
1008 Gobbi, A., Mantese, N., Zuecco, G., Borga, M., Bonazza, M., Sobotková, M.,
1009 Čejková, B. and Wassenaar, L.I.: Technical Note: Evaluation of between-sample
1010 memory effects in the analysis of δ2H and δ18O of water samples measured by laser
1011 spectroscopes, Hydrol. Earth Syst. Sci., 16, 3925–3933, doi:10.5194/hess-16-3925-
1012 2012, 2012.

1013 Penna, D., Engel, M., Mao, L., dell'Agnese, A., Bertoldi, G. and Comiti, F.: Tracer-based
1014 analysis of spatial and temporal variations of water sources in a glacierized catchment,

Hydrol. Earth Syst. Sci., 18, 5271–5288, doi:10.5194/hess-18-5271-2014, 2014.

Penna, D., van Meerveld, H.J., Zuecco, G., Dalla Fontana, G., Borga, M.,: Hydrological response of an Alpine catchment to rainfall and snowmelt events. Journal of Hydrology 537, 382–397. https://doi.org/10.1016/j.jhydrol.2016.03.040, 2016.

Penna, D., Engel, M., Bertoldi, G., and Comiti, F.: Towards a tracer-based conceptualization of meltwater dynamics and streamflow response in a glacierized catchment, Hydrol. Earth Syst. Sci., 21, 23–41, 10.5194/hess-21-23-2017, 2017a.

Penna, D., Zuecco, G., Crema, S., Trevisani, S., Cavalli, M., Pianezzola, L., Marchi, L., Borga, M.: Response time and water origin in a steep nested catchment in the Italian Dolomites: Response time and water origin in a nested catchment. Hydrological Processes 31, 768–782. https://doi.org/10.1002/hyp.11050, 2017b.

Peralta-Tapia, A., Sponseller, R. A., Ågren, A., Tetzlaff, D., Soulsby, C., and Laudon, H.: Scale-dependent groundwater contributions influence patterns of winter baseflow stream chemistry in boreal catchments, J. Geophs. Res. Biogeo., 120, 847-858. doi:10.1002/2014JG002878, 2015.

R Core Team: R: A Language and Environment for Statistical Computing. R Foundation for Statistical Computing, Vienna, Austria, 2016.

Ragettli, S., Immerzeel, W.W., and Pellicciotti, F.: Contrasting climate change impact on river flows from high-altitude catchments in the Himalayan and Andes Mountains, Proc. Natl. Acad. Sci., 113, 9222–9227, doi:10.1073/pnas.1606526113, 2016.

Ragettli, S., and Pellicciotti, F.: Calibration of a physically based, spatially distributed hydrological model in a glacierized basin: On the use of knowledge from glaciometeorological processes to constrain model parameters, Water Resour. Res., 48, 1–20, doi:10.1029/2011WR010559, 2012.

Rinaldo, A., Benettin, P., Harman, C.J., Hrachowitz, M., Mcguire, K.J., Velde, Y. Van Der, Bertuzzo, E., Botter, G.: Storage selection functions: A coherent framework for quantifying how catchments store and release water and solutes, Water Resourses Res. 51, doi:10.1002/2015WR017273, 2015.

Rogger, M., Chirico, G.B., Hausmann, H., Krainer, K., Brückl, E., Stadler, P., Blöschl, G.: Impact of mountain permafrost on flow path and runoff response in a high alpine catchment, Water Resour. Res., 53 (2), 1288–1308, 2017.

Roy, J.W., and Hayashi, M.: Multiple, distinct groundwater flow systems of a single moraine–talus feature in an alpine watershed, J. Hydrol., 373, 139–150, doi: 10.1016/j.jhydrol.2009.04.018, 2009.

Rutter, N., Hodson, A., Irvine-Fynn, T., and Solås, M.K.: Hydrology and hydrochemistry of a deglaciating high-Arctic catchment, Svalbard, J. Hydrol. 410, 39–50, doi:10.1016/j.jhydrol.2011.09.001, 2011.

Schaefli, B., Maraun, D. and Holschneider, M.: What drives high flow events in the Swiss Alps? Recent developments in wavelet spectral analysis and their application to hydrology, Adv. Water Resour., 30, 2511–2525, doi:10.1016/j.advwatres.2007.06.004, 2007.

Schmieder, J., Marke, T., and Strasser, U. Tracerhydrologische Untersuchungen im Rofental (Ötztaler Alpen / Österreich). Innsbrucker Jahresbericht, Institut für Geographie der Universität Innsbruck, 109 – 120, 2017.

Schwarb, M.: The Alpine Precipitation Climate. Swiss Federal Institut of Technology Zurich, 2000.

Shevchenko, V. P., Pokrovsky, O. S., Vorobyev, S. N., Krickov, I. V., Manasypov, R. M., Politova, N. V., Kopysov, S. G., Dara, O. M., Auda, Y., Shirokova, L. S., Kolesnichenko, L. G., et al.: Impact of snow deposition on major and trace element concentrations and fluxes in surface waters of Western Siberian Lowland, Hydrol. Earth Syst. Sci, 21, 5725–5746, doi:10.5194/hess-2016-578, 2016.

Sicart, J.E., Pomeroy, J.W., Essery, R.L.H., Bewley, D.: Incoming longwave radiation to melting snow: Observations, sensitivity and estimation in northern environments. Hydrol. Process. 20, 3697–3708, doi:10.1002/hyp.6383, 2006.

Sicart, J. E., Hock, R. and Six, D.: Glacier melt, air temperature, and energy balance in different climates: The Bolivian Tropics, the French Alps, and northern Sweden, J. Geophys. Res., 113, 1–11, doi: 10.1029/2008JD010406, 2008.

1072 Singh, P., Haritashya, U.K., Ramasastri, K.S., and Kumar, N.: Diurnal variations in discharge
1073 and suspended sediment concentration, including runoff-delaying characteristics, of
1074 the Gangotri Glacier in the Garhwal Himalayas, Hydrol. Process., 19, 1445–1457,
1075 doi:10.1002/hyp.5583, 2005.

1076 Sivapalan, M.: Prediction in ungauged basins: a grand challenge for theoretical hydrology,
1077 Hydrol. Process. 17, 3163–3170, doi:10.1002/hyp.5155, 2003

1078 Sklash, M. G., R. N. Farvolden, and Fritz, P.: A conceptual model of watershed response to
1079 rainfall, developed through the use of oxygen-18 as a natural tracer, Can. J. Earth Sci.,
1080 13, 271-283, 1976.

1081 Smiraglia, C., GLIMS Glacier Database. Boulder, CO. National Snow and Ice Data Center.
1082 http://dx.doi.org/10.7265/N5V98602, 2015.

1083 Soulsby, C., Tetzlaff, D., Dunn, S. M. and Waldron, S.: Scaling up and out in runoff process
1084 understanding: Insights from nested experimental catchment studies, Hydrol. Process.,
1085 20, 2461–2465, doi: 10.1002/hyp.6338, 2006a.

1086 Soulsby, C., Tetzlaff, D., Rodgers, P., Dunn, S. and Waldron, S.: Runoff processes, stream
1087 water residence times and controlling landscape characteristics in a mesoscale
1088 catchment: An initial evaluation, J. Hydrol., 325, 197–221, doi:
1089 10.1016/j.jhydrol.2005.10.024, 2006b.

1090 Sprenger, M., Leistert, H., Gimbel, K. and Weiler, M.: Illuminating hydrological processes at
1091 the soil-vegetation-atmosphere interface with water stable isotopes, Rev. Geophys.,
1092 54, 674–704, doi:10.1002/2015RG000515, 2016.

1093 Staudinger, M., Stoelzle, M., Seeger, S., Seibert, J., Weiler, M. and Stahl K.: Catchment water
1094 storage variation with elevation, Hydrol. Process., 31, 2000–2015, doi:
1095 10.1002/hyp.11158, 2017.

1096 Stingl, V. and Mair, V.: An introduction to the geology of South Tyrol. Autonome Provinz
1097 Bozen, Amt für Geologie und Baustoffprüfung, Kardaun (BZ), 80 S., 2005.

1098 Swift, D. A., Nienow, P. W., Hoey, T. B. and Mair, D. W. F.: Seasonal evolution of runoff
1099 from Haut Glacier d'Arolla, Switzerland and implications for glacial geomorphic
1100 processes, J. Hydrol., 309, 133–148, doi:10.1016/j.jhydrol.2004.11.016, 2005.

1101 Taylor, S., Feng, X., Kirchner, J.W., Osterhuber, R., Klaue, B. and Renshaw, C.E.: Isotopic
1102 evolution of a seasonal snowpack and its melt, Water Resour. Res. 37: 759–769.
1103 DOI:10.1029/2000WR900341, 2001.

1104 Tetzlaff, D., Seibert, J., McGuire, K. J., Laudon, H., Burns, D. A., Dunn, S. M. and Soulsby,
1105 C.: How does landscape structure influence catchment transit time across different
1106 geomorphic provinces, Hydrol. Process., 23, 945–953, 2009.

1107 Tetzlaff, D., Buttle, J., Carey, S.K., McGuire, K., Laudon, H., and Soulsby, C.: Tracer-based
1108 assessment of flow paths, storage and runoff generation in northern catchments: a
1109 review, Hydrol. Process., 29, 3475–3490, doi: 10.1002/hyp.10412, 2014.

1110 Thies, H., Nickus, U., Mair, V., Tessadri, R., Tait, D., Thaler, B. and Psenner, R.: Unexpected
1111 response of high Alpine Lake waters to climate warming, Environ. Sci. Technol., 41,
1112 7424–9, 2007.

1113 Thies, H., Nickus, U., Tolotti, M., Tessadri, R., Krainer, K., Evidence of rock glacier melt
1114 impacts on water chemistry and diatoms in high mountain streams, Cold Reg. Sci.
1115 Technol., 96, 77–85, doi:10.1016/j.coldregions.2013.06.006, 2013.

1116 Uhlenbrook, S. and Hoeg, S.: Quantifying uncertainties in tracer-based hydrograph
1117 separations : a case study for two- , three- and five-component hydrograph separations
1118 in a mountainous catchment, Hydrol. Process., 17, 431–453, doi:10.1002/hyp.1134,
1119 2003.

1120 U.S. Army Corps of Engineers: Summary Report of the Snow Investigations, Snow
1121 Hydrology , North Pacific Division, Portland, Oregon, 1956.

1122 Vaughn, B. H. and Fountain, A. G.: Stable isotopes and electrical conductivity as keys to
1123 understanding water pathways and storage in South Cascade Glacier, Washington,
1124 USA, Ann. Glaciol., 40, 107–112, doi: 10.3189/172756405781813834, 2005.

1125 Vincent, C. and Six, D.: Relative contribution of solar radiation and temperature in enhanced
1126 temperature-index melt models from a case study at Glacier de Saint-Sorlin, France,
1127 Ann. Glaciol., 54(63), 11–17, doi:10.3189/2013AoG63A301, 2013.

1128 Viviroli, D., Archer, D.R., Buytaert, W., Fowler, H.J., Greenwood, G.B., Hamlet, A. F.,
1129 Huang, Y., Koboltschnig, G.R., Litaor, M.I., López-Moreno, J.I., Lorentz, S.,

Schädler, B., Schreier, H., Schwaiger, K., Vuille, M., and Woods, R.: Climate change and mountain water resources: overview and recommendations for research, management and policy, Hydrol. Earth Syst. Sci., 15, 471–504, doi:10.5194/hess-15-471-2011, 2011.

Weiler, M., Seibert, J. and Stahl, K.: Magic components - why quantifying rain, snow- and icemelt in river discharge isn't easy, Hydrol. Process., doi:10.1002/hyp.11361, 2017.

Williams, M.W., Knauf, M., Caine, N., Liu, F., Verplanck, P.L.: Geochemistry and source waters of rock glacier outflow, Colorado Front Range, Permafr. Periglac. Process., 17, 13–33, doi:10.1002/ppp.535, 2006.

Williams, M.W., Hood, E., Molotch, N.P., Caine, N., Cowie, R., and Liu, F.: The 'teflon basin' myth: hydrology and hydrochemistry of a seasonally snow-covered catchment, Plant Ecol. Divers., 8, 639-661, doi:10.1080/17550874.2015.1123318,2015.

Wolfe, P.M. and English, M.C.: Hydrometeorological relationships in a glacierized catchment in the Canadian high Arctic, Hydrol. Process., 9, 911–921, doi: 10.1002/hyp.3360090807, 1995.

Wolock, D. M., Fan, J., and Lawrence, G. B.: Effects of basin size on low-flow stream chemistry and subsurface contact time in the Neversink River watershed, New York, Hydrol. Process., 11, 1273-1286, 1997.

Wu, X.: Diurnal and seasonal variation of glacier meltwater hydrochemistry in Qiyi glacierized catchment in Qilian mountains, northwest china: Implication for chemical weathering, J. Mt. Sci., 15, 1035-1045, doi:10.1007/s11629-017-4695-2, 2018.

Xing, B., Liu, Z., Liu, G., Zhang, J.: Determination of runoff components using path analysis and isotopic measurements in a glacier-covered alpine catchment (upper Hailuogou Valley) in southwest China, Hydrol. Process., 29, 3065–3073, doi:10.1002/hyp.10418, 2015.

Zhou, S., Wang, Z. and Joswiak, D. R.: From precipitation to runoff: stable isotopic fractionation effect of glacier melting on a catchment scale, Hydrol. Process., 28, 3341–3349, doi: 10.1002/hyp.9911, 2014.

Zuecco, G., Carturan, L., De Blasi, F., Seppi, R., Zanoner, T., Penna, D., Borga, M., Carton,

A., and Della Fontana, G.: Understanding hydrological processes in glacierized catchments: Evidence and implications of highly variable isotopic and electrical conductivity data, Hydrol. Process., 33: 816–832, doi: 10.1002/hyp.13366, 2018.

Zuecco, G., Penna, D., Borga, M., and van Meerveld, H. J.: A versatile index to characterize hysteresis between hydrological variables at the runoff event timescale, Hydrol. Process, 30, 1449–1466. doi:10.1002/hyp.10681, 2016.

Zuzel, J.F., and Cox, L.M.: Relative importance of meteorological variables in snowmelt, Water Resour. Res., 11, 174–176, 1975.

1168 Table 1. Meteorological characteristics of the weather station Madritsch/Madriccio 2.825 m
1169 a.s.l. in 2014 and 2015.

Date	2014	2015
Precipitation (total / rain / snow) (mm y^{-1})*	1284/704/579	961/637/323
Mean annual air temperature (°C)	-1.4	-0.8
Days with maximum daily air temperature > 6.5 / 15 °C	74 / 0	99 / 15
Days with snow cover > 10cm	270	222
Maximum snow depth (date)	02/03/2014	27/03/2015
Maximum snow depth (cm)	253	118
Date of snow cover disappearance	12/07/2014	13/06/2015
Median discharge (m^3 s^{-1})	9.5	5.2

1170 * Precipitation data are not wind-corrected. Rain vs. snow separation was performed
1171 following Auer (1974)
1172

1173 Table 2. Topographical characteristics of sub-catchments defined by sampling points.

Sampling point	Description	Catchment area (km^2)	Glacier extent (2011)* (%)	Elevation range
T1	Trafoi River	51.28	16.5	1587 - 3469
T2	Trafoi River	46.72	18.1	1404 - 3889
T3	Trafoi River	12.18	26.9	1197 - 3889
TT1	Tributary draining Trafoi glacier	4.32	18	1587 - 3430
TT2	Small creek	0.05	0	1607 - 2082
TT3	Tributary draining Zirkus/ Circo glacier	6.46	34.6	1605 - 3888
TSPR1	Spring at the foot of a slope	-	0	1602**
TSPR2	Spring at the foot of a slope	-	0	1601**
S1	Sulden River	130.14	13	1109 - 3896
S2	Sulden River	74.61	11.1	1296 - 3896
S3	Sulden River	57.01	14.9	1707 - 3896
S4	Sulden River	45.06	17.8	1838 - 3896
S5	Sulden River	18.91	19.2	1904 - 3896
S6	Sulden River	14.27	38.5 / 14.8	2225 - 3896
ST1	Razoi tributary	6.46	0	1619 - 3368
ST2	Zay tributary	11.1	8.1	1866 - 3543
ST3	Rosim tributary	7.3	11.6	1900 - 3542

SSPR1	Spring in the valley bottom near Sulden town	-	0	1841*
SSPR2 - 4	At the base of the rock glacier front	-	0.12***	2614, 2594, 2600*

* the glacier extent refers to Smiraglia (2015).

** for spring locations, the elevation of the sampling point is given.

*** for rock glacier spring locations, the glacier cover refers to the extent of both rock glaciers.

Table 3. Nivo-meteorological indicators derived from the weather station Madritsch/Madriccio at 2825 m a.s.l..

Variable	Unit	Description
P_{1d}	mm	Cumulated precipitation of the sampling day
P_{nd}		Cumulated precipitation n days prior to sampling day
T_{max1d}	°C	Maximum air temperature during the sampling day
T_{maxnd}		Maximum air temperature within n days prior to sampling day
G_{max1d}	W/m²	Maximum global solar radiation during sampling day
G_{maxnd}		Maximum global solar radiation within n days prior to sampling day
ΔSD_{1d}	cm	Difference of snow depth measured at the sampling day at 12:00 and the previous day at 12:00, based on 6h averaged snow depth records.
ΔSD_{nd}		Difference of snow depth measured at the sampling day at 12:00 and n days prior the sampling day at 12:00, based on 6h averaged snow depth records.
D_{Prec1}	days	Days since last daily cumulated precipitation of > 1mm was measured.

D_{Prec10}		Days since last daily cumulated precipitation of > 10mm was measured.
D_{Prec20}		Days since last daily cumulated precipitation of > 20mm was measured.

Table 4. Variability coefficient (VC) for selected locations along the Sulden and Trafoi River in 2014 and 2015.

Location	River section (in km)	VC
T3	6.529	0.70
T2	2.774	0.85
T1	51	1.09
S6	12.87	0.01
S3	6.417	0.42
S2	2.739	0.35
S1	0	0.77

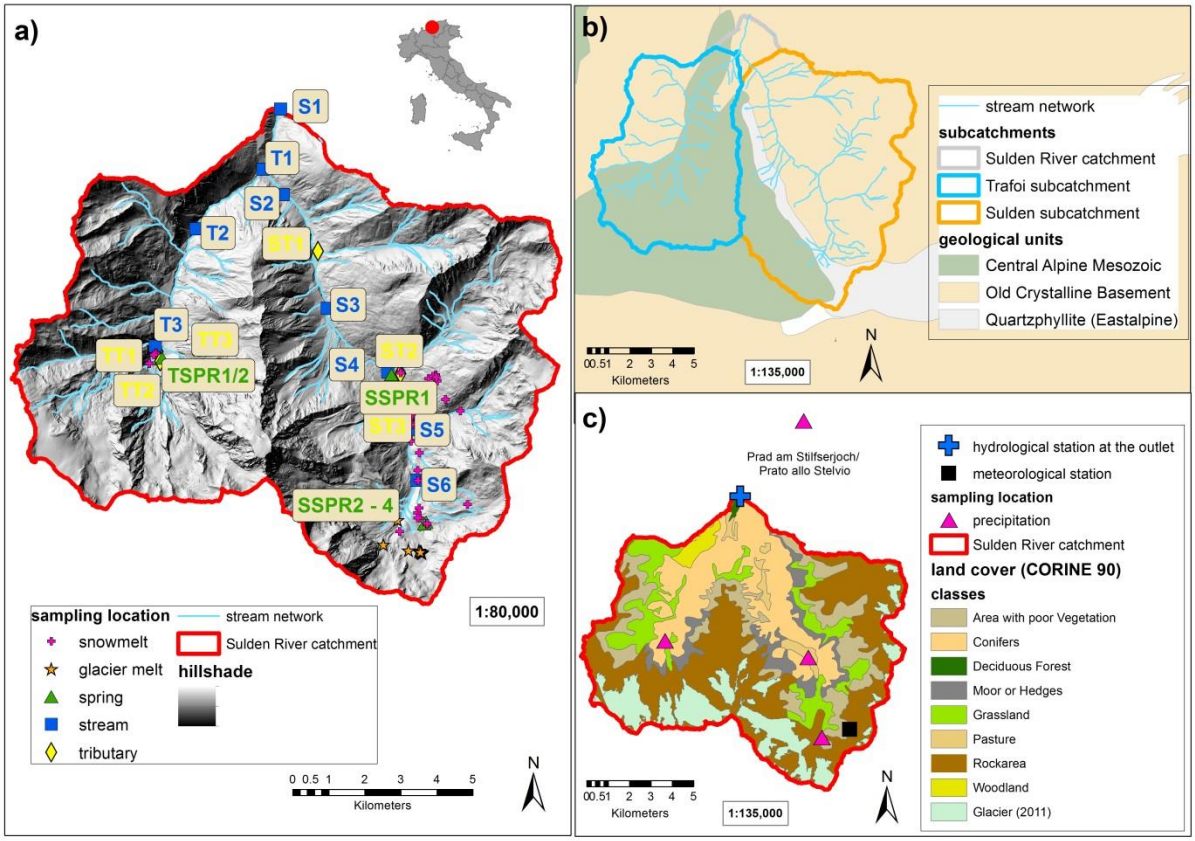

Figure 1. Overview of the Sulden catchment with a) sampling point, b) geology, and c) land cover with instrumentation. The meteorological station shown is the Madritsch/Madriccio AWS of the Hydrographic Office (Autonomous Province of Bozen-Bolzano). The glacier extent of 2011 is based on Smiraglia (2015).

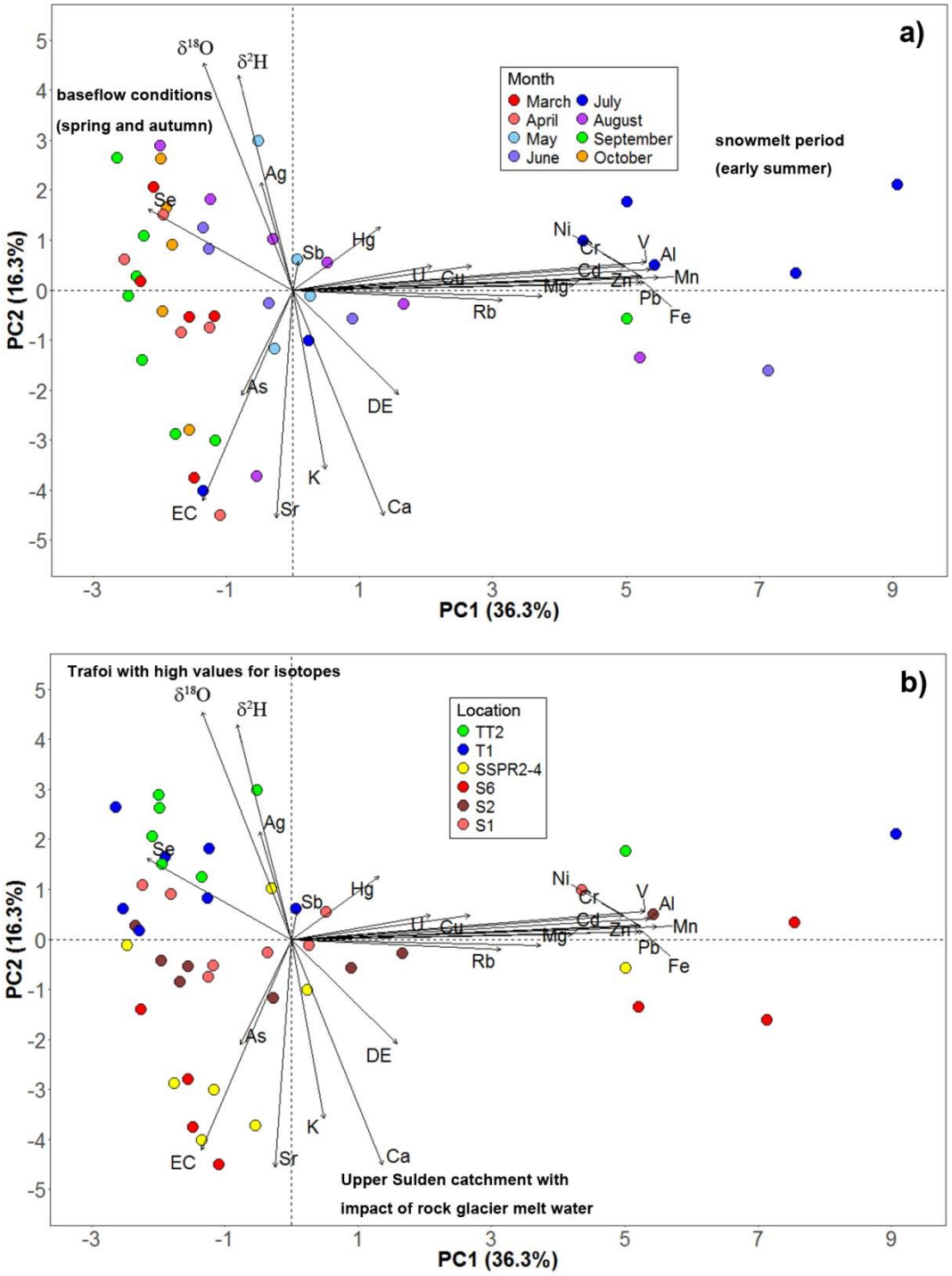

Figure 2. Principle component analysis of element concentrations of stream water and springs draining a rock glacier sampled in the Sulden and Trafoi sub-catchments from March to October 2015. Data based on n = 47 samples are shown in groups according to a) the sampling locations and b) the sampling month.

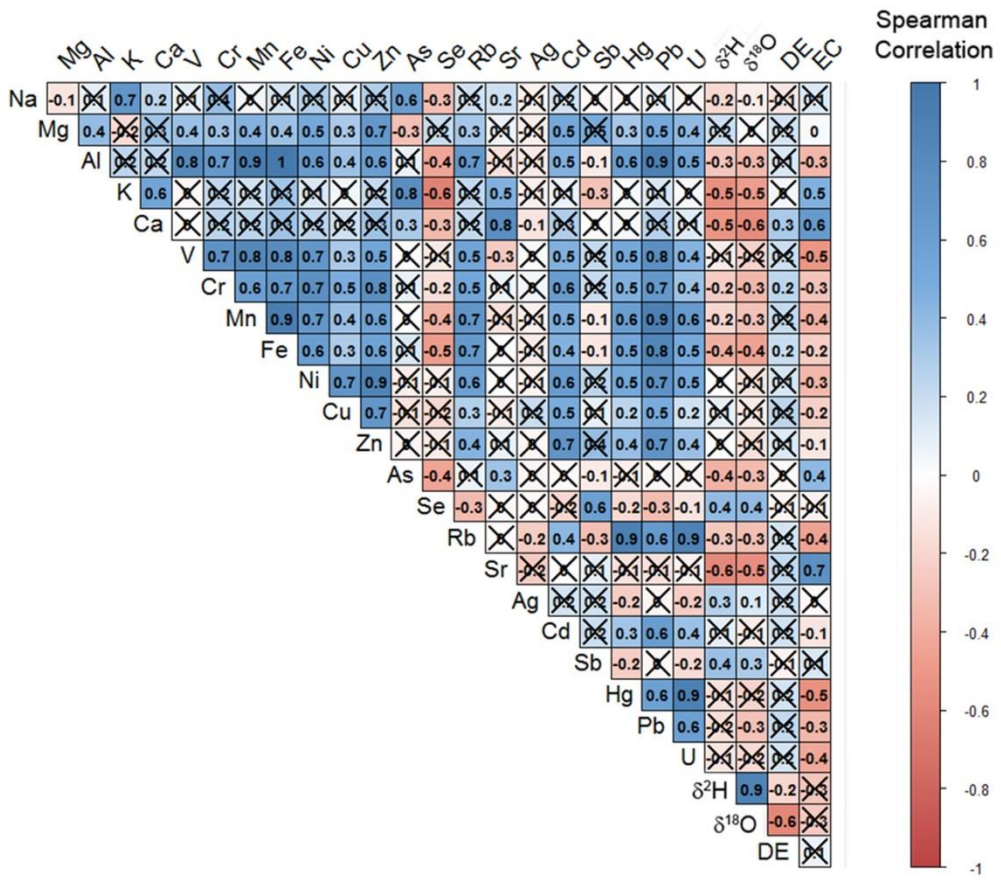

Figure 3. Spearman rank correlation matrix of hydrochemical variables. Values are shown for a level of significance *p* < 0.05, otherwise crossed out.

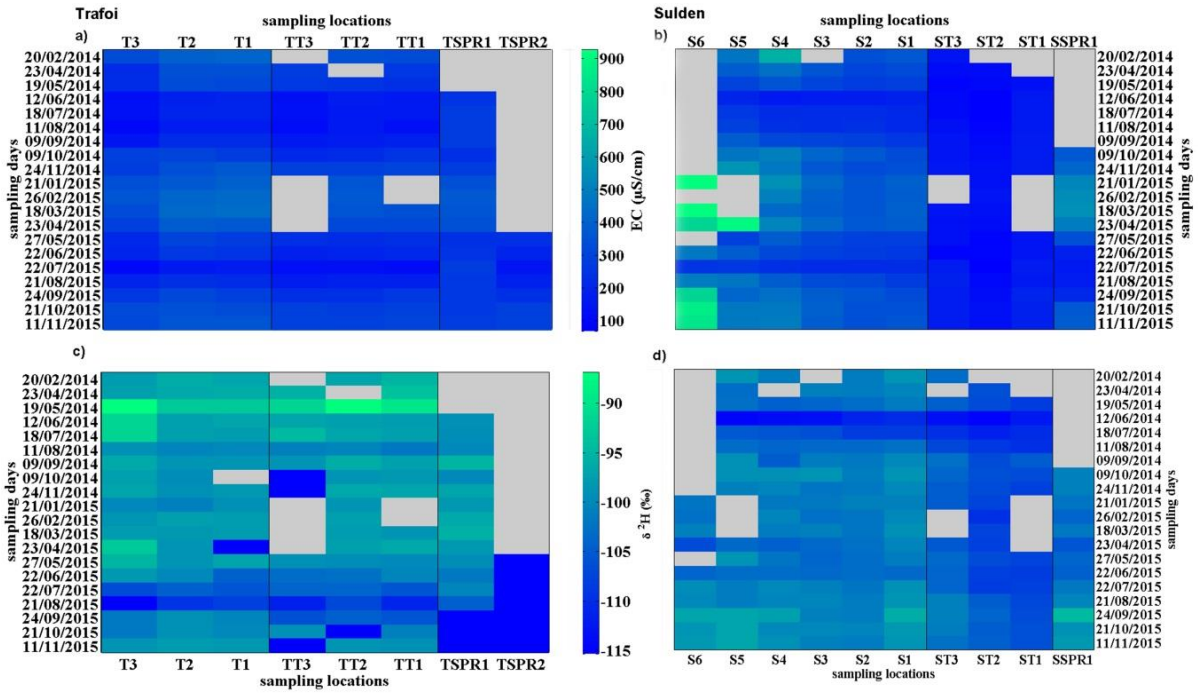

Figure 4. Spatial and temporal variability of EC (µS cm^{-1}) and δ²H (‰) at different stream sections, tributaries and springs within the Trafoi sub-catchment (subplot a and c) and the Sulden sub-catchment (subplot b and d) in 2014 and 2015. The heatmaps are grouped into locations at streams, tributaries, and springs. Grey areas refer to missing sample values due to frozen or dried out streams/tributaries or because the sampling location was included later in the sampling scheme.

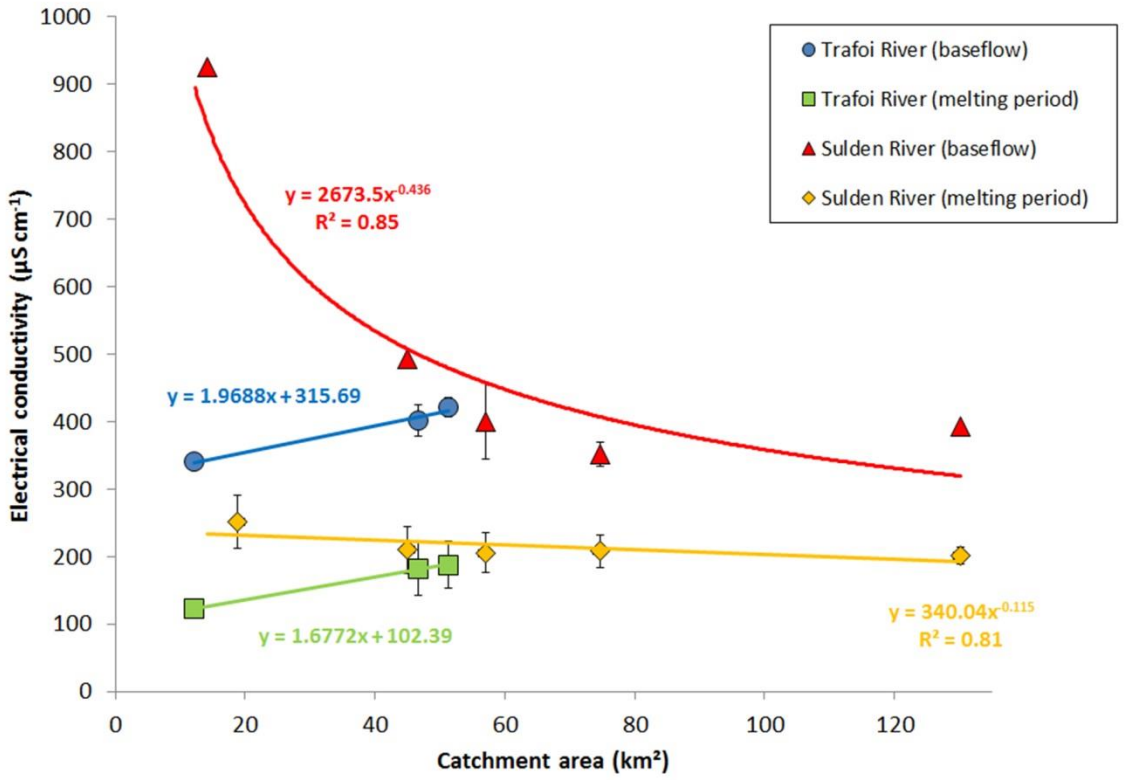

Figure 5. Spatial variability of electrical conductivity along the Trafoi and Sulden River against catchment area. Electrical conductivity is averaged for sampling days during baseflow conditions (21/01/2015, 26/02/2015, and 18/03/2015) and melting period (12/06/2014, 18/07/2014, 11/08/2014, and 09/09/2014).

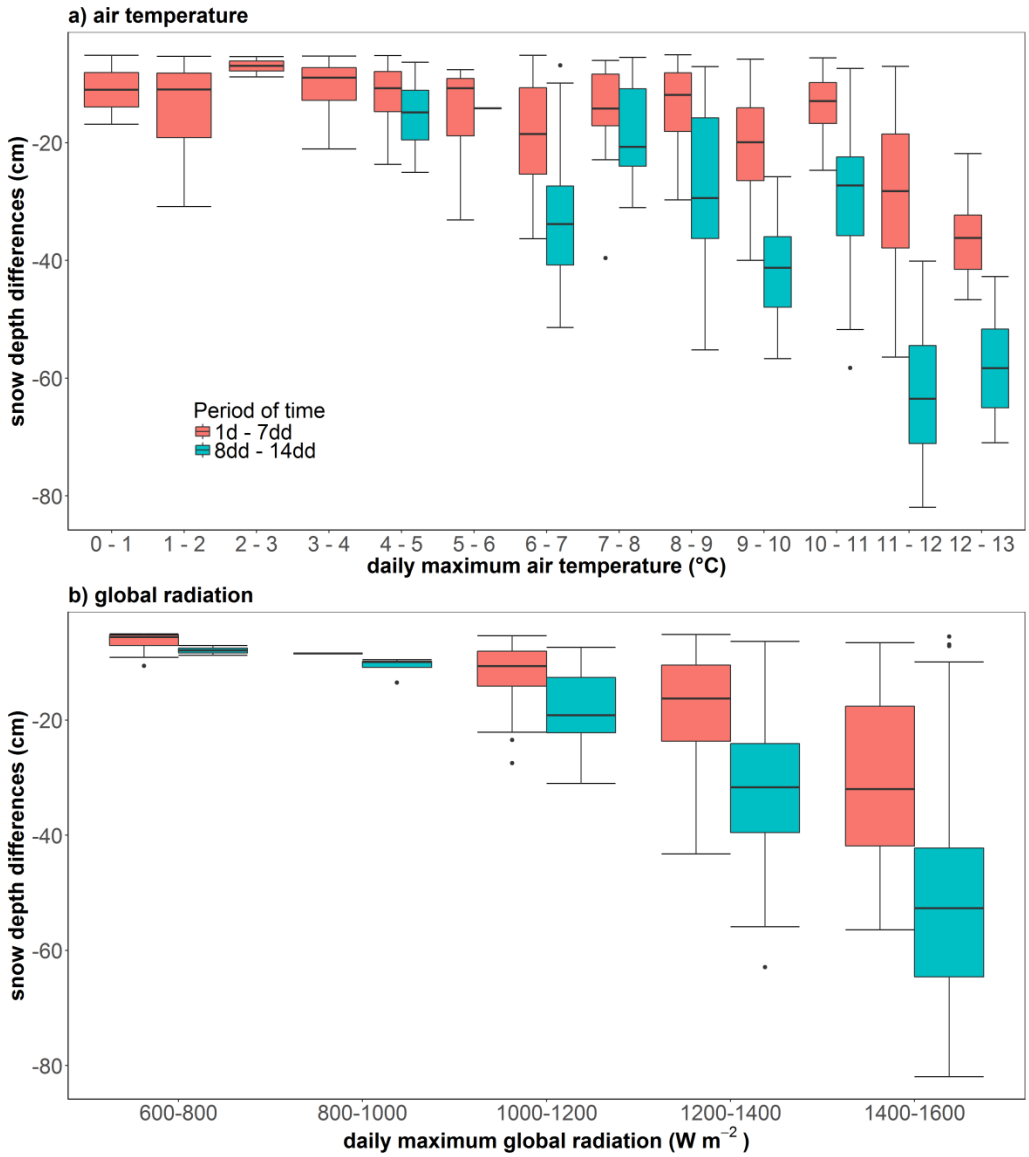

Figure 6. Box-plots of environmental variables a) daily maximum air temperature and b) daily maximum global radiation on snowmelt expressed as snow depth differences at AWS Madritsch. Snow depth differences smaller than 5 cm are discarded from analysis.

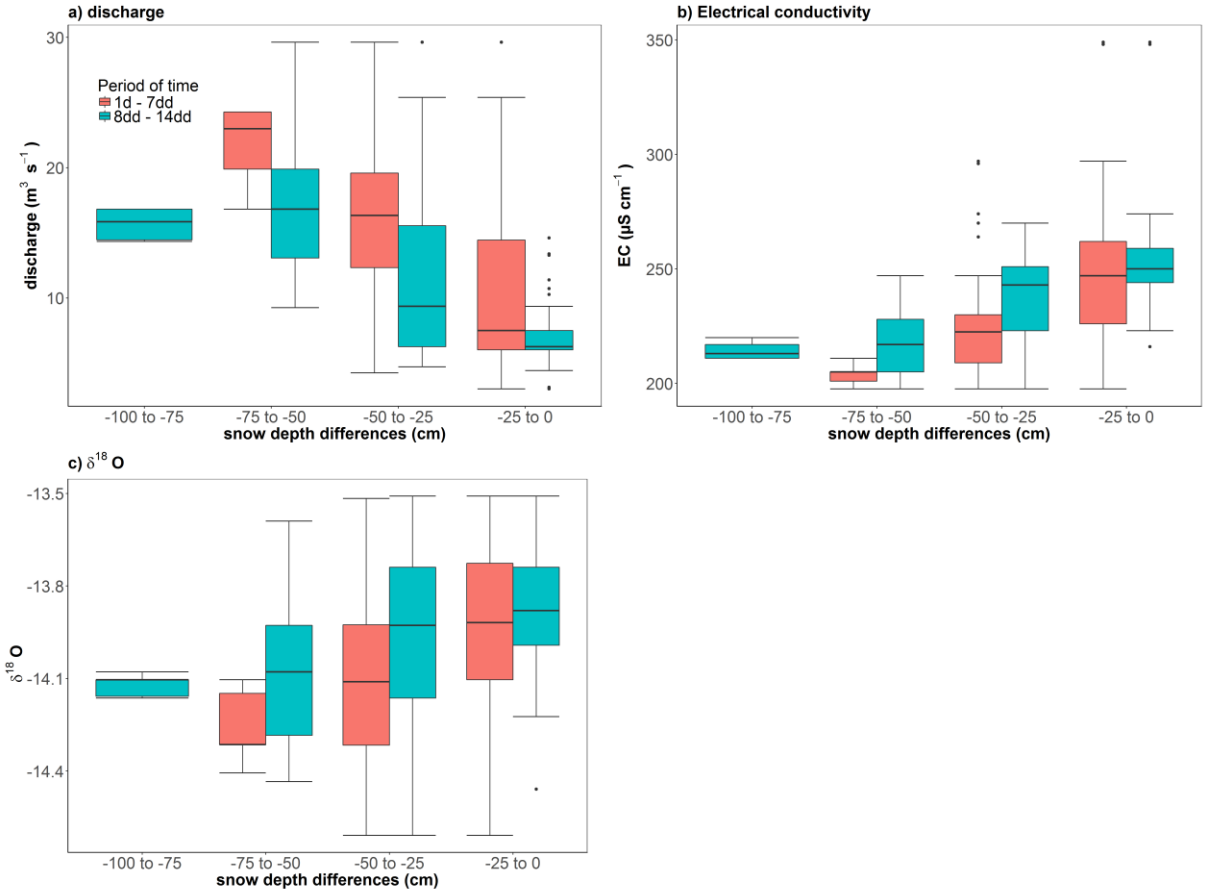

Figure 7. Box-plots of snowmelt expressed as snow depth differences at AWS Madritsch on the variability of a) discharge, b) EC, and c) $\delta^{18}O$ at the outlet Stilfserbrücke in 2014 and 2015.

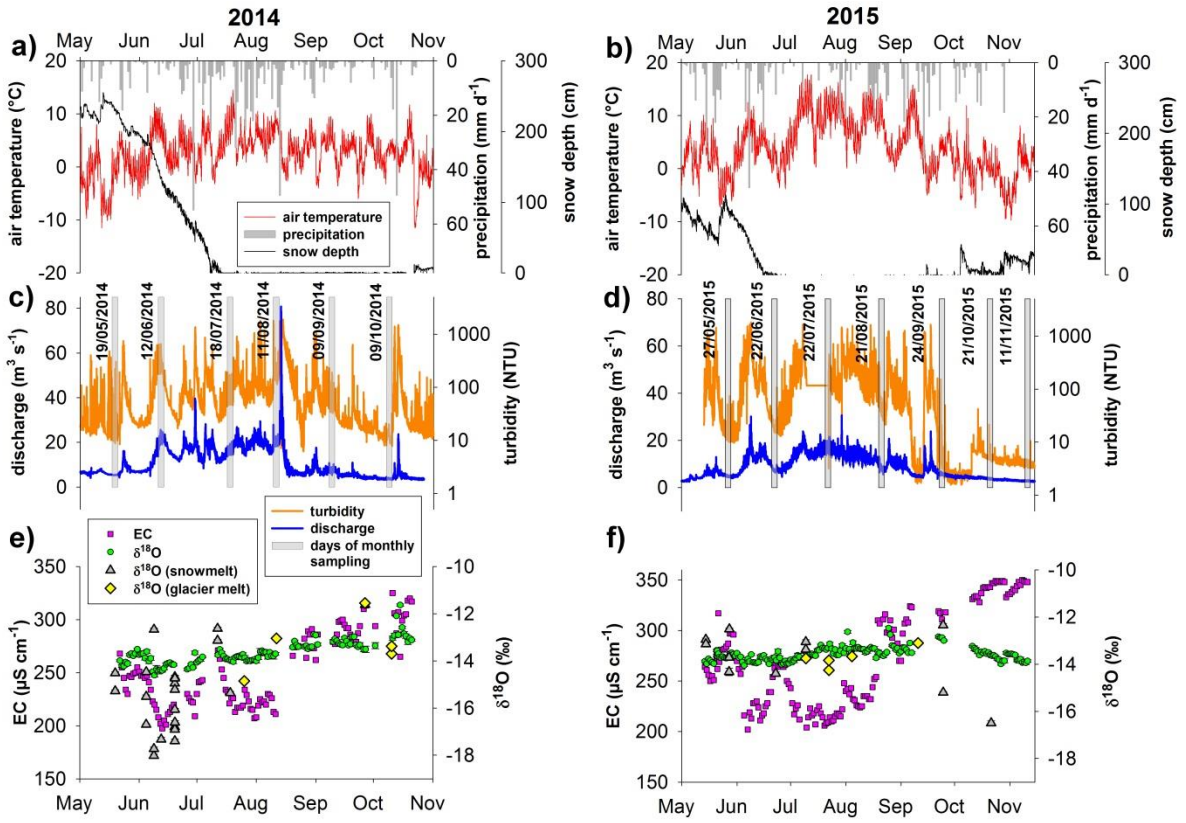

Figure 8. Time series from 2014 and 2015 of a) and b) precipitation, hourly air temperature and snow depth at the AWS Madritsch, c) and d) streamflow and turbidity, e) and f) electrical conductivity and $\delta^{18}O$ of the stream at the outlet Stilfserbrücke and of snowmelt and glacier melt water. Grey shaded bars indicate the date of monthly sampling carried out in the entire catchment.

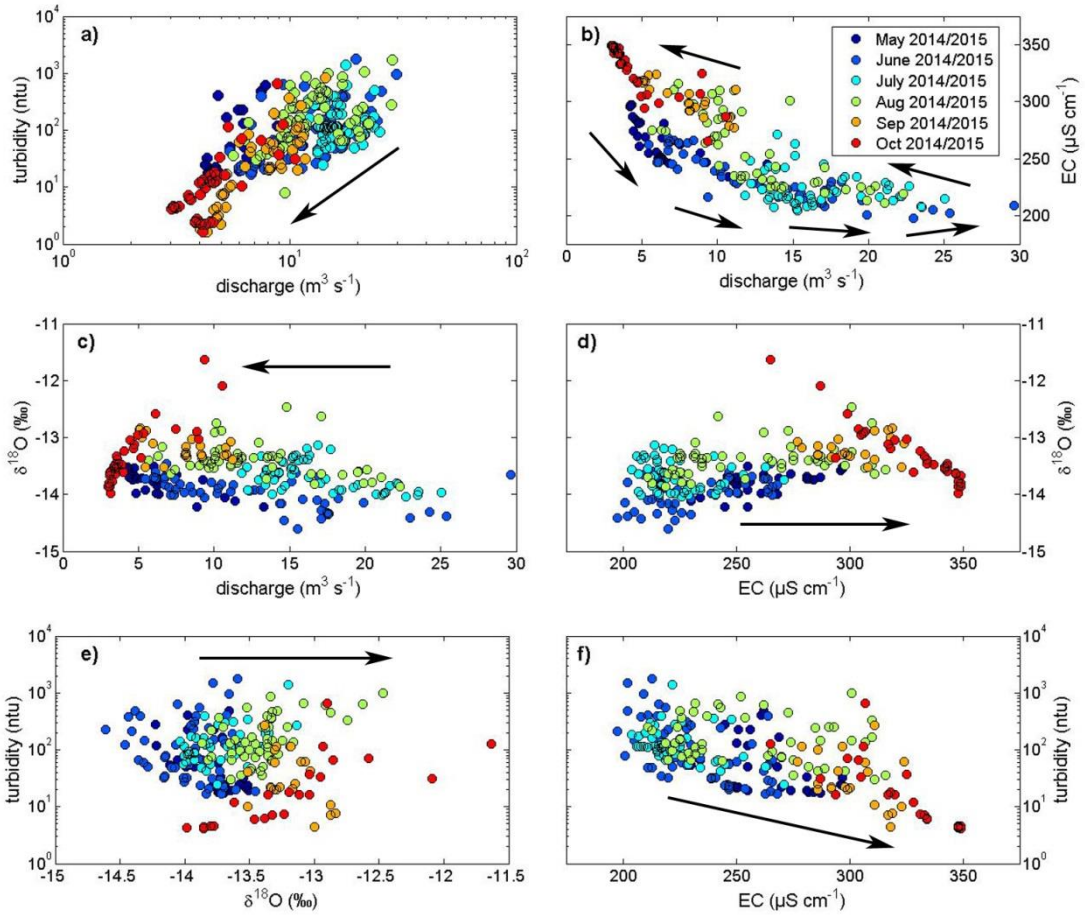

Figure 9. Monthly relationships between a) to e) discharge, turbidity and tracers such as EC and $\delta^{18}O$ at the outlet Stilfserbrücke in 2014 and 2015. The dataset consists of n = 309 samples. Arrows underline the monthly pattern.

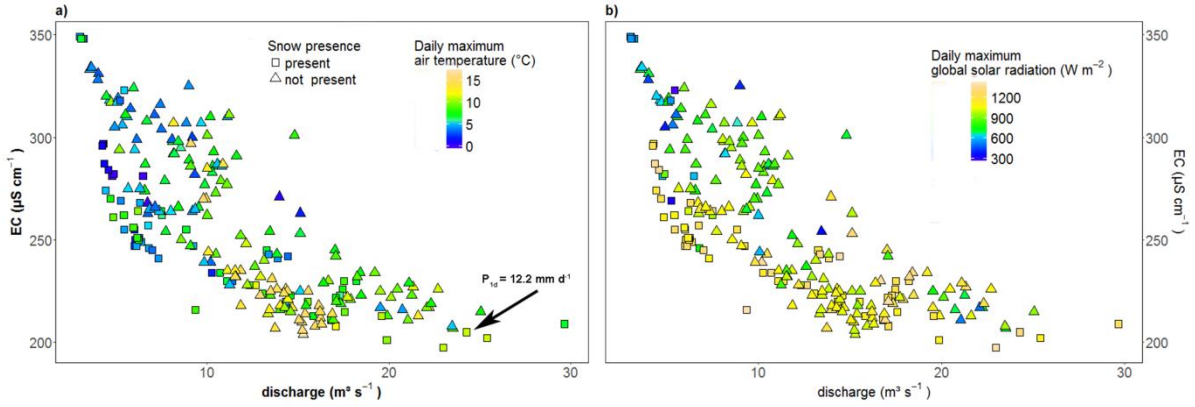

Figure 10. Monthly relationships between discharge and electrical conductivity (EC) at the outlet Stilfserbrücke with respect to a) daily maximum air temperature (1d) and b) daily maximum global solar radiation (1d) compared to the snow presence measured at the AWS Madritsch in 2014 and 2015.